Lunds Universitets Naturgeografiska Institution

Seminarieuppsatser Nr. 84

Arctic aerosol and long-range transport

In collaboration with:
Department of Physical Geography, Lund University and
The Institute of Applied Environmental Research (ITM), Air Pollution Laboratory, Stockholm University

Jessica Umegård

2001

Department of Physical Geography,
Lund University
Sölvegatan 13, S-221 00 Lund,
Sweden

Abstract

Aerosols have been measured at the Zeppelin station, at Ny-Ålesund, Svalbard, from March 2000 to April 2001. Two instruments were used, a Condensation Particles Counter and a Differential Mobility Particle Sizer, which measured total aerosol number density above 0.02 μm as well as the aerosol size distribution between 0.02 μm and 0.621 μm in diameter. The results have been analyzed with help of 10-day back-trajectories in order to find possible source areas for the characteristic aerosol types.

The particle number concentration in the Arctic shows distinct annual variation. It is highest in summer and lowest in winter. The aerosol volume and surface also show a minimum in winter. The highest aerosol volume and surface was found in spring. A smaller effective diameter, i.e. a larger fraction of small particles was found in summertime compared to winter.

The air mass back trajectories calculated for the altitude of 500 m. a.s.l. indicated a seasonal pattern depending on particle size. Episodes with a higher fraction of large particles and with high aerosol surface and volume mostly occurred in winter and spring. The air masses during these episodes are predominantly originating from the east. Frequent occasions with large number concentrations of small particles are present in the summer. These occasions are though not associated with large volume or surface. The preferred air mass origin during these episodes is from west.

Sammanfattning

Under ett år, från mars 2000 till april 2001, samlades data om arktiska aerosoler in på mätstationen Zeppelin, Ny-Ålesund, Svalbard. Två instrument användes, en Condensation Particles Counter och en Differential Mobility Particle Sizer som mätte aerosoler i storleks intervallet 0.02-0.621 μm. Resultatet har analyserats och utvärderats med hjälp av 10 dagars baklänges trajektorier för att söka tänkbara källområden för olika karakteristiska luft massor med avseende på olika typer av aerosol egenskaper

Maximum för partikel antalet inträffade under sommaren medan vintern uppvisade betydligt lägre koncentrationer. Våren visade på högre aerosol volym och yta än under resten av året. Lägsta värdena för dessa parametrar var under vintern. Den uträknade effektiva parametern som säger något om andelen stora eller små partiklar, visar på låga värden under sommaren. Detta innebär att vi troligast har många små partiklar under sommaren, medan vi på vintern har få men i medeltal större partiklar.

Trajektorier för luftmassor på 500 meters höjd visar på ett säsongsbundet mönster beroende på partikel storlek. Vid tillfällen med större andel stora partiklar och med mer aerosol volym och yta kommer luften oftare från öst. Dessa förhållanden är vanligast under våren och vintern. Tillfällen med höga koncentrationer av små aerosoler, vanligtvis förekommande under sommaren, visade på luftmassor ursprungligen västerifrån.

Table of content

1. Introduction

For a long time the Arctic was supposed to be one of the last places still undisturbed by man's activities. While it is one of the world's last, large, mainly undisturbed terrestrial ecosystems, the Arctic now faces problems due to climate change, ozone depletion, long-range transported pollution and unsustainable use. According to the Intergovernmental Panel on Climate Change [*IPCC*, 1996] the most uncertain part of the anthropogenic climate forcing is the effect of atmospheric aerosol. Atmospheric aerosol particles influence the Earth radiation balance both directly by scattering and absorbing solar radiation, and indirectly by acting as cloud condensation nuclei.

The rapid movement of air makes the atmosphere an important pathway for delivering contaminants to the Arctic. Any chemically stable, wind-borne material will follow winds and weather patterns into and within the Arctic region. Precipitation occurs through out the year in the Arctic and scavenges very efficiently the ambient aerosol. Over a larger scale in space and time, this sink must be balanced by a source of particles resulting in a typical number density of a few hundred particles per cubic centimetre. The source may be in-suit production of new particles or imported through transport of particles from the lower latitudes.

The objective of the proposed work is to study the Arctic aerosol and relate its properties to the air mass history with special emphasis on the long-range transport. The data is interpreted with respect to the preferential origin of the air mass when different types of aerosol loading are observed. We ask the question: Is it possible to identify geographical areas based on air mass origin where the aerosol properties observed at Ny-Ålesund, Svalbard, present a systematic feature? For instance, is the presence of small newly formed particles associated with preferential air mass trajectories, or is the presence of large aerosol surface area only a result of the advection of anthropogenic pollution into the Arctic basin?

Questions such as these are important in understanding the aerosol life cycle in a remote region like the Arctic. Occasionally, air from lower latitudes enters into the Arctic and effectively acts as a source of particles into this reservoir. In spring this phenomena is particularly strong and is termed Arctic Haze. This is a well-known phenomenon with very strong influence from anthropogenic sources on the Arctic air composition. Our intention is too study not only very obvious events, as the Arctic Haze, but also more subtle, but important, intrusions that may occur throughout the whole year.

1.2 Theoretical background

The atmosphere is a thin layer of air surrounding the Earth. This thin layer is a complex and dynamic mixture of particles and gases, which is of greatest importance for life on Earth. The presence of gases like ozone, oxygen, carbon dioxide, and water vapour, create some of the necessary conditions for life. Further, the ozone protects organisms from ultraviolet sunlight and plays an important role in the Earth energy budget.

A large amount of energy is continuously transferred from the Sun to the Earth by the sunlight. About a third of the incoming power (343 W/m^2) is reflected, and the rest, (240 W/m^2), is absorbed by the ground and the atmosphere, as can be seen in fig. 1, [*Ahrens*, 1994]. In equilibrium situation the amount of energy brought to the Earth by sunlight is

balanced by the heat losses from the Earth through the infrared radiation to space. Several gases occurring naturally in the atmosphere absorb infrared light, which is randomly re-emitted some of course back towards the ground. Clouds play a major role in the Earth's radiation balance by trapping both visible light and infrared light. [*Brimblecombe*, 1996].

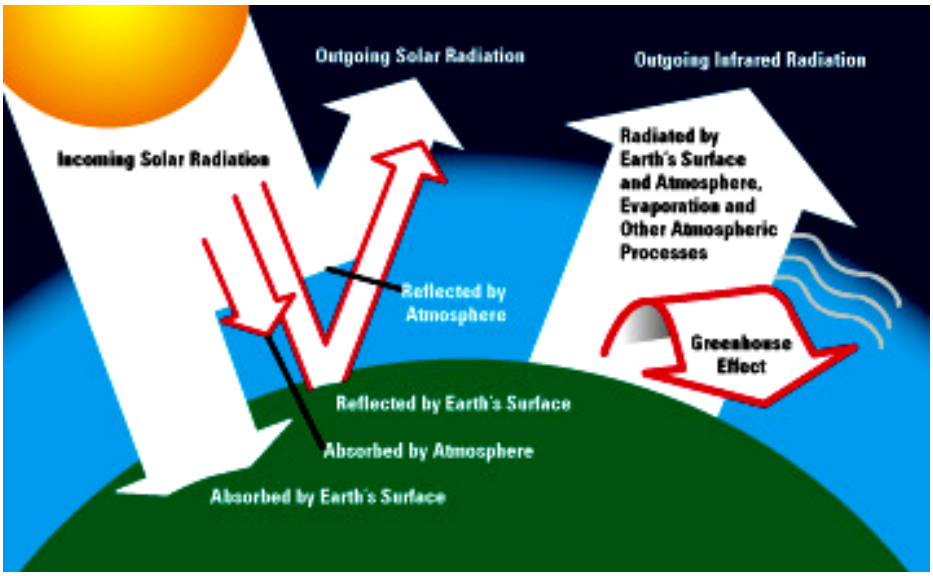

Fig. 1. Earth's overall energy balance, [Internet 1]. Net input of solar radiation must be balanced by net output of infrared radiation. About one-third of incoming solar radiation is reflected and the remainder is mostly absorbed by the surface.

The atmosphere and its components are constantly in motion. The driving force of the atmospheric circulation is the difference in temperature between low and high latitudes. A deficit in energy at the poles must be balance by a transport of energy from the tropics where the insulation from the Sun causes a surplus of energy. The surface of the Earth absorbs more energy than the air above. Hence, a vertical transport of energy also takes place. In the process of balancing the energy on the planet, winds are generated, clouds are formed, and precipitation produced. This is what we usually call weather [*Oke*, 1987].

To evaluate the dynamics of relatively long-lived trace species, the average exchange of mass between the Northern and Southern Hemispheres and vertically are sometimes represented as transfers among well-mixed compartments. It takes about 1 to 3 months to mix species throughout a hemisphere, whereas between 1 and 2 years are needed to mix species through the entire Earth's lower atmosphere. The relatively long time for mixing between the Northern and Southern Hemispheres arises from the presence of the Inter Tropical Convergence Zone (ITCZ) near the Equator. Because air rises in this zone, the region has considerable cloudiness and rain and no strong north-south winds that would tend to mix gases between the Northern and Southern Hemispheres. Dispersion of materials occurs more efficient in the summer by horizontal winds, while in the winter, vertical transport tends to predominate, [*Strahler*, 1992].

1.2.1 Aerosols

The microscopic particles that are present in the air are of many kinds: for example resuspended soil particles, smoke from power generation, photochemically formed particles,

salt particles formed from ocean spray, and atmospheric clouds of water droplets or ice particles. Theses airborne particles are all examples of aerosols, and they vary greatly in their ability to affect not only visibility and climate but also our health and quality of life. An aerosol is defined in its simplest form as a collection of solid or liquid particles suspended in a gas, and they are natural as well as anthropogenic. Natural sources of aerosols are for example forest fires, erosion, sea spray, and the oceanic DMS, which is oxidized to the sulphate in the atmosphere. Among the anthropogenic sources, the use of fuels for heating, electric power production and transportation are very important. Industrial processes can also cause emissions of aerosol particles, or gases that can be converted into particles [*Oke*, 1987].

The principal reasons for any monitoring of particles in the atmosphere can be divided into three categories: **health effects**, **atmospheric chemistry**, and **cloud/climate interactions**. The effects on health are both direct, via deposition of aerosols in the lungs and indirect, for example via acid deposition to the soil, making heavy metals more available to plants that are used as food. By changing the chemical environment, deposited aerosols can have great effect on the ecosystem. The soil Ph has been reduced due to sulphuric acid, nitric acid and related compounds, which to a great extent are brought to the ecosystem as aerosol particles. Changes like this can lead to some species being favored, on the behalf of others. The particles affects the climate as they scatter and absorb radiation, and serve as airborne collection and reaction surfaces for atmospheric trace gases. By scatter incoming visible light, they thereby prevent some of the sunlight from reaching the ground, causing cooling. The scattering efficiency depends on the particle size, with the highest cross section per particle volume in the diameter range 0.5-1μm. Aerosol particles act as condensation nuclei in all cloud and precipitation processes, and thereby have an indirect effect on the climate. A higher number concentration of cloud droplets, resulting from an increased concentration of tropospheric condensation nuclei, increases the cloud reflectivity and thereby the cooling effect of Earth. A decrease in cloud droplet size can lead to a lower probability for precipitation and changes in life times for clouds [*Svenningsson*, 1997].

The residence time of the aerosol has important implications with regard to the transport and distribution of substances associated with particulate matter. The residence time of the aerosols is depending on their size, but also on cloud appearance and soluble material in the particle. Tropospheric aerosols have a residence time between a few hours up to a few weeks, whereas the vertical transport, between surface and tropopause, takes about a month. The average residence time for aerosol particles in the troposphere decreases from 1 week to a couple of days, when the particle diameter increases from 1 to 10μm and for 100μm particles the residence time is only about one hour. Since the residence time is shorter than the time constant for vertical transport, an efficient process is needed for the removal of particles from the troposphere. A low deposition rate is a condition for the atmospheric transport of aerosols over long distances [*Warneck*, 1988].

1.2.2 Sources and sinks

There are two main sources of fine particles in the atmosphere, primary and secondary. The primary particulate material is directly derived from dispersal of solids from the Earth's surface and from the ocean. The secondary particulate material forms because of chemical reactions in the atmosphere. Several processes influence the formation and growth of particles; the most common ones are nucleation, condensation and coagulation. Nucleation form new particles from gas phase material. Particles may grow by condensation, which describes the deposition of vapor-phase material onto particulate matter. Coagulation is the

process where collisions between two or more particles lead to the formation of a new particle of larger size. Since at normal humidities most particles are sheathed with a liquid layer, the sticking probability is assumed to be unity. Collisions between two particles thus lead to the formation of a new particle of larger size [*Warneck*, 1988].

The chemical content of the aerosol varies considerably between different sites and time, but also with particle size. On a global scale, the aerosol can schematically be divided into three types: the continental, the maritime, and the tropospheric background aerosol. By chemical composition, the first two types contain mainly materials from the nearby surface sources, somewhat modified by the coagulation of particles of different origin and by condensation products resulting from gas-phase reactions. The third type represents an aged and much diluted continental aerosol. This type is present also at the surface of the ocean. In general, the particles in the coarse fraction ($d>1$ μm) contain components from soil and seawater, mainly primary material that is mechanically produced. Anthropogenic sources contribute mainly to the coarse fraction of the aerosol only close to the source. The fine fraction ($d< 1$ μm) is formed by liquid phase reactions, by products from chemical reactions in the atmosphere and condensable vapours. Both in polluted and more clean areas, the fine fraction of the aerosol is to a large extent made up of the secondary aerosol components, such as sulphates and nitrates [*Svenningsson*, 1997].

All kinds of aerosols are subject to various removal mechanisms; among the most important ones is deposition, which removes the aerosol mass from the atmosphere. Deposition of the atmospheric particles takes place via both dry and wet processes. Wet deposition includes precipitation scavenging in which particles are deposited in rain and snow, when fog, cloud-water, and mist intercept the surface. Dry deposition is the direct transfer of particles to the ground, through sedimentation, impaction or diffusion. Dry deposition is considered more effective for coarse particles and elements such as iron and manganese, whereas wet deposition generally is more effective for fine particles and elements such as cadmium, lead and nickel [*Brimblecombe*, 1996].

1.2.3 Aerosol Size Distribution

In an aerosol particle distribution several modes, first proposed by Whitby, [*Whitby*, 1978], with different characteristics, can be identified. In fig. 2 a particle volume distribution shows the different modes and some of the processes controlling them.

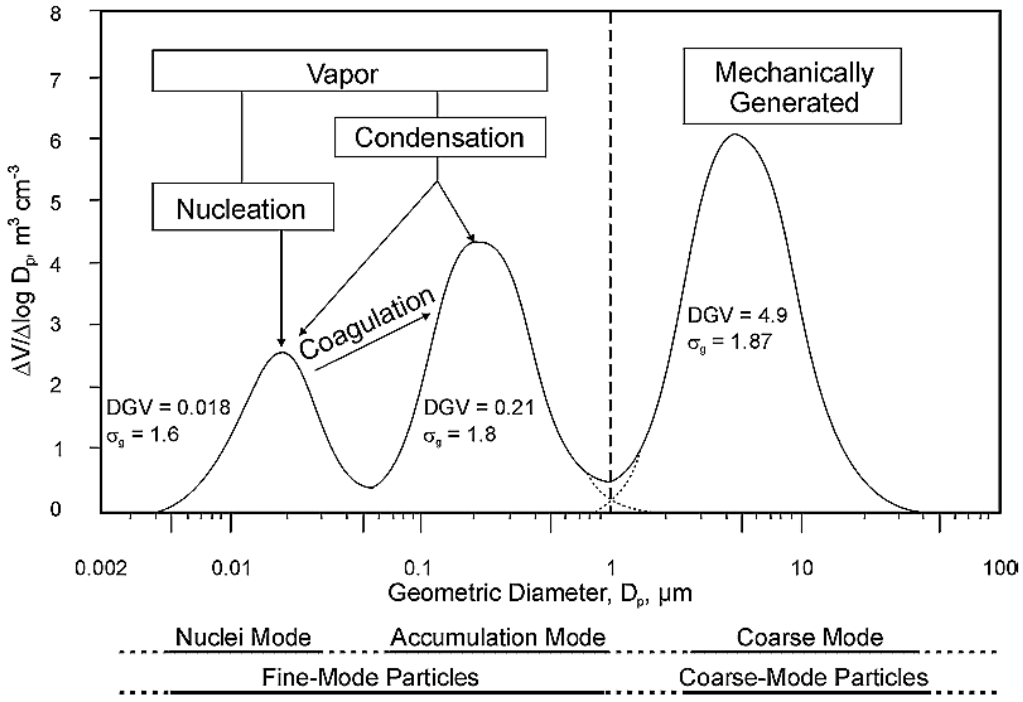

Fig. 2. In a particle volume distribution different modes can be identified; nuclei mode with a diameter up to 0.06µm, accumulation mode between 0.06-1 µm and coarse mode particles larger than 1 µm, [Internet 2].

Nuclei mode particles are the smallest, with a diameter less than about 0.06 µm. They are mainly formed by homogeneous nucleation of vapours following chemical reactions, or changes in temperature or relative humidity. They may also grow when gases condense upon pre-existing particles with low vapour pressure. The concentration of the nuclei particles varies strongly with source and sink strengths. In clean air masses, nucleation may rapidly form many nuclei particles, whereas in air masses containing larger aerosols coagulation will remove them. The accumulation mode particles, particles with a diameter between 0.06-1 µm, can be activated to cloud drops and gain a considerable mass due to liquid phase oxidation of sulphur. For particles that act as cloud condensation nuclei, mainly accumulation mode particles and the largest nuclei mode particles, precipitation is an important deposition mechanism. Due to their low total deposition rate, the nuclei and accumulation mode particles have long residence times in the atmosphere. The coarse particles have diameters larger than about 1 µm and they have different sources and chemical composition compared to the fine fraction. Because of their large size, the coarse particles readily settle out from the atmosphere or impact on surfaces, so their lifetime in the atmosphere is only a few hours or days. Due to their high deposition rate through interception, impaction and sedimentation, the concentration of particles in the coarse fraction varies strongly with the wind speed, the structure of the ground and the distance to large sources, [*Warneck*, 1988].

1.2.4 Physical properties

Characterization of aerosols involves considerable difficulties due to the fact that the aerosol properties vary rapidly in space and time. Each particle is characterized by many parameters, for example size, shape, density, refraction index and chemical composition. The parameters most relevant to measure depend on the question that is asked.

All properties of aerosols depend on particle size, and most aerosols cover a wide range of sizes; a hundred-fold or thousand-fold range between the smallest and largest particles of an aerosol is common. Size is difficult to define for atmospheric particles, because usually we do not know their shape. Often they are treated as spheres, because the terminal velocity of small spheres, ν_t, is easily derived from Stokes' Law, [*Warneck*, 1988]:

$$\nu_t = 2d\rho_p g/(9\nu) \qquad (1)$$

Where: ν the velocity of the fluid
ρ_p is the density of the particle.
d is the diameter
g is the gravidity

Particle size is most commonly refer to as particle diameter with the given symbol *d*. Particle density refers to the mass per unit volume of the particle itself, usually expressed in kg m^{-3} [g cm^{-3}]. The mass concentration is the most commonly measured aerosol property, which is the mass of particulate matter in a unit volume of aerosol. The aerosol number concentration, N, is the number of particles per unit volume of aerosol, [*Warneck*, 1988].

Measurements of particulate in the atmosphere are normally displayed in terms of a size distribution function. This function is often seen plotted as the number concentration over a given size range. If the size range of the interval is made very small then the number concentration can be written as the differential:

Number concentration= $dN/d \log (Dp)$ (2)

Likewise, the size distribution according to particle surface and particle volume can be expressed by the equations:

Surface: $dS/d \log (Dp)= 4\pi d^2 \, dN/d \log (Dp)$ (3)

Volume: $dV/d \log (Dp)=(4\pi/3)d^3 \, dN/ d \log (Dp)$ (4)

An example of distribution functions is shown in figure 3. It is seen that the number concentration peaks, in the smaller size range. In contrast to number concentration, which is dominated by nuclei particles, aerosol surface and volume are determined primarily by the accumulation particles respectively the coarse particles, [*Warneck*, 1988].

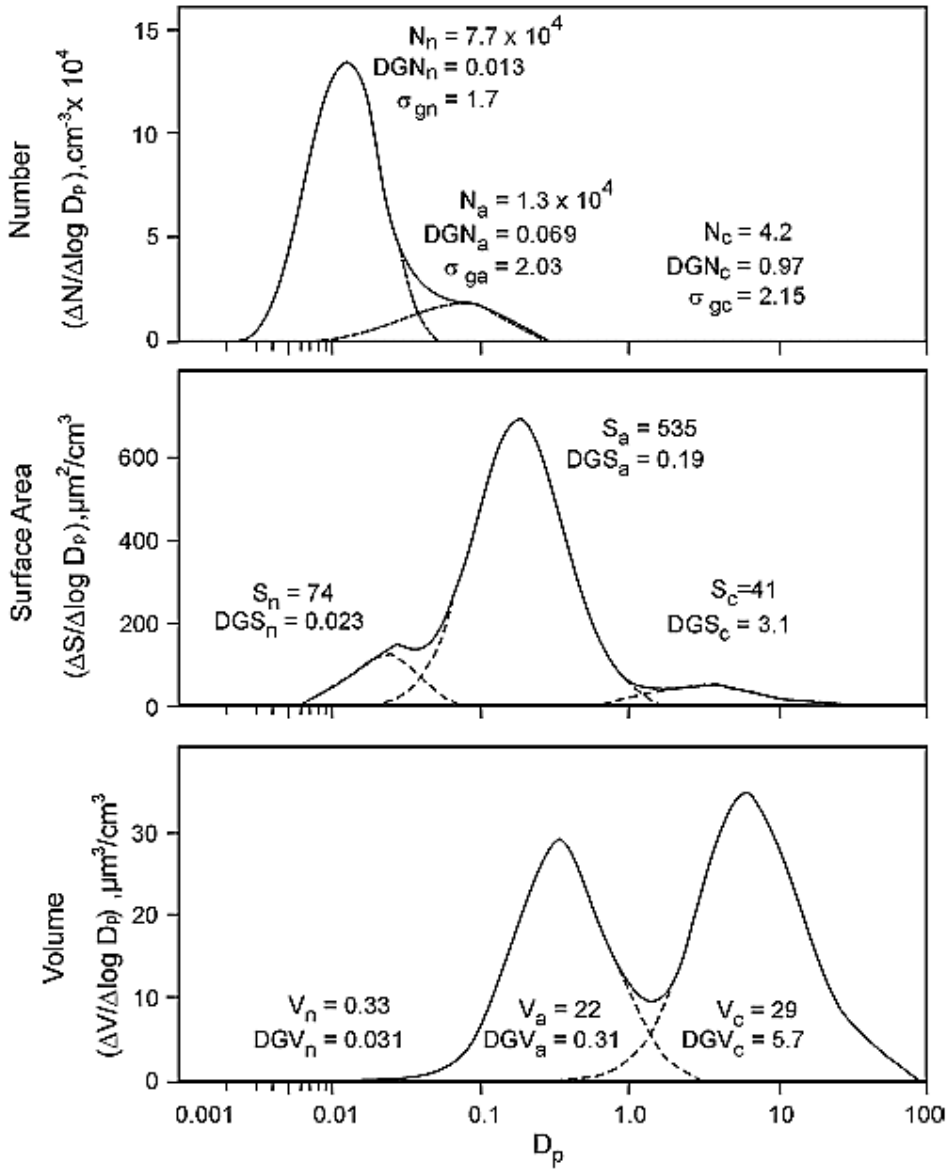

Fig. 3. Diagrams of a number distribution, surface distribution, and volume distribution, [Internet 2].

1.3 The study area – the Arctic

The Arctic is primarily an adjective vaguely synonymous with "far northern". In climatic terms the Artic is the northern region in which, according to Köppen's definition, the mean temperature of the warmest month does not exceed 10° C, [*Strahler*, 1992]. Precipitation in the Arctic is generally low with a summer maximum, even though high wintertime snowfall may occur in mountains and glaciated areas due to orographic effects. Most of the 17-million km^2 north of 75° N are permanently covered with pack ice. The Artic lies in the polar easterlies, with a mean atmospheric transport from east to west. Winds over the Arctic basin are generally light and variable. The atmosphere is dry and precipitation is overall low but higher over Greenland, Svalbard and islands of the Barents Sea, where the relatively warm moist air from the north Atlantic brings snowfall enough to maintain icecaps. Despite its dryness the air is often close to saturation; inversions and radiation fogs occur frequently, especially over settlements and open water. Wind patterns and precipitation in the Arctic are

governed by the low-pressure systems that form over the North Atlantic and the Bering Sea, bringing warm, moist air northward. These weather systems, the Icelandic and Aleutian lows, gather moisture over open water and dump it as precipitation when the air is forced to rise. The windward sides of mountainous areas often have daily rain or snow. In the warm seasons, the Icelandic and Aleutian lows weaken considerably [*Rey*, 1982].

On Svalbard´s west coast, fig. 4, Ny-Ålesund (79° N, 12°E) has been called a "natural laboratory" due to its location in an undisturbed Arctic environment. The Svalbard islands are close both to the intense cyclonic activity in the North Atlantic and to the Polar Basin. Observations in this area are therefore particularly valuable in studies of the meteorological conditions governing air pollution transport into the Arctic. The Zeppelin Mountain at Ny-Ålesund is an excellent site for atmospheric monitoring, with minimal contamination from the local settlement due to its location at 474 m.a.s, which sometimes is above the inversion layer. The weather on Svalbard can shift very quickly and local variations are often considerable. In Longyearbyen (the main settlement on Svalbard), the seasonal average temperature ranges from -14°C during the winter to +6°C during the summer. Despite Svalbard being close to the North Pole, the islands have a relatively mild climate compared to other areas at the same latitude. During the summer it is common with periods of fog. In terms of precipitation, Svalbard may be described as an "Arctic desert" with annual rainfall at a mere 200-300 mm [*Rey*, 1982].

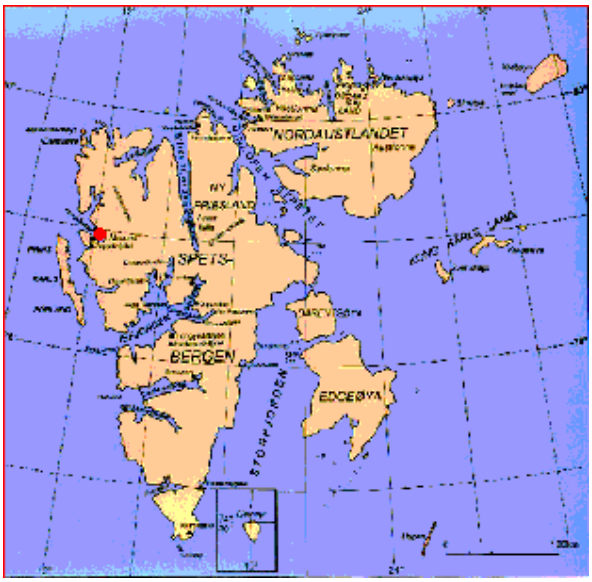

Fig. 4. A map of Svalbard. Ny-Ålesund is situated on the west coast, and is marked with a red dot, [Internet 3].

1.3.1 The Arctic aerosol

Arctic aerosols have been investigated in a number of physical and chemical studies [*Xie et al.*, 1999b], [*Baskaran*, 2001], [*Khattatov et al.*, 1997]. There is a general consensus that there is a difference between winter and summer conditions; the mass concentration of aerosols is high in winter and low in summer. The reason for the strong seasonal variations may be due to a varying pattern of atmospheric transport and different atmospheric lifetimes of the aerosols under winter and summer conditions.

Air-transport patterns are highly dependent on season and on the position of the major weather systems. Rahn's coupling/decoupling hypothesis explains the winter/summer differences in aerosol concentration by an annual variation in northern hemisphere circulation, [*Heintzenberg*, 1985]. Figure 5 shows the Arctic front situation in summer and winter. In winter and spring, an intense high-pressure system over Siberia pushes the Arctic front far to the south, so that important polluted areas of Eurasia are actually within the Arctic air mass, the lower one-to-two kilometres of which can move contaminants across the pole. The transport of contaminants during the Arctic winter is made effective by the lack of clouds and precipitation over the areas dominated by high-pressure systems. Low wind speeds and temperature inversions, caused by the cold winter weather, allow contaminants to accumulate in the atmosphere,[*Heintzenberg*, 1985]. Dry deposition rates for snow-covered surfaces are also small. Rather than falling to the ground in the vicinity of the source the aerosol follow the large-scale patterns of atmospheric circulation. The low level circulation and the meridional exchange of air are also more intense in the winter-spring season, [*Ottar*, 1986].

Fig. 5. The position of the Arctic front influences contaminant transport in the atmosphere. The figure shows the mean position of Arctic air mass in January and July and the winter and summer frequencies of winds driving the major south-to-north transport routes, [Internet 4].

The atmospheric removal processes are much more efficient in summer than in winter. In summer persistent stratus clouds, which act as efficient wet aerosol scrubbers, are covering large parts of the Arctic. Precipitation occurs by fog or drizzle from these low stratus clouds, resulting in rapid removal of aerosols and water-soluble gases. Concentrations of anthropogenic pollutants are also lower in summer than in winter, which is partly explained by above named decoupling of the Arctic from the source regions [*Pacyna and Ottar*, 1985]. Summer is also warmer, allowing for cloud formation and for drizzling rain that can remove contaminants from the air before they are carried far. Moreover, sunlight during the summer

months allows for photochemical degradation of some contaminants and converting into particles.

The summer Arctic troposphere is often pictured as an aerosol sink region with wet scavering processes in the boundary layer eliminating the particulate matter that is imported at preferred altitudes. In contrast to the frequent transport from mid-latitude source regions in winter, summer pollution enters the Artic infrequently. Therefore, the transport of air and contaminants from mid-latitudes becomes much less important in summer than in winter [*Heintzenberg et al.*, 1991].

The polar aerosol contains among others; carbonaceous material from midlatitude pollution sources, sulfate, sea salt from the surrounding ocean, and mineral dust from arid regions at lower latitudes [*Seinfeld*, 1998]. Detailed measurements show that the winter arctic pollution aerosols mainly consist of ammonium sulphate and sulphuric acid droplets with a narrow size distribution between 0.1 and 0.5 μm. This is typical of an aged atmospheric aerosol, which has been produced by condensation and coagulation from gaseous precursors [*Ottar*, 1986]. During the late winter and early spring, the Arctic aerosol has found to be significantly influenced by anthropogenic sources, and the phenomena is commonly referred to as Arctic Haze, [*Seinfeld*, 1998].

1.3.2 Arctic Haze

While up to the middle of last century, air pollution was generally regarded as a local problem in large cities and industrial areas, it is today evident that man-made emissions are gradually changing the chemistry of the whole atmosphere, even on continental and global scales. For a long time the Arctic was supposed to be one of the last places still undisturbed by man's activities. In the 1950´s an unusual reduction in visibility in the Arctic was observed wintertime. At an early stage, windblown dust from the great Asian deserts was believed to be a major component, but continued studies left no doubt that the Arctic haze consists mainly of man-made air pollutants [*Ottar*, 1986].

Arctic haze is predominantly a boundary layer phenomenon, i.e. by far most of the pollution burden is confined to the lowermost two kilometres of the atmosphere. The most frequent altitude with a relative maximum is about 1.5 km, which corresponds closely to the 850 mb pressure level, at which empirical studies locate most of the long-range transport of air pollution from boundary layer sources. The aerosol contains soil particles and various trace metals, which can be used as chemical fingerprints to pinpoint emission sources [*Heintzenberg*, 1985].

One of the striking features of Arctic haze is its seasonal variation. Both the optical effects of the haze and the concentration of its major constituents have a strong winter-spring maximum and summer minimum. The intensity of the haze, as expressed by its optical depth, or turbidity, is several times greater in spring than in summer. Because of the generally low scavenging rates and reduced photochemistry in the Arctic, the haze can persist for long periods of time [*Radke et al.*, 1984]. The most severe episodes occur when stable high-pressure systems produce clear, calm weather, and the visibility can be reduced to 30 kilometres, in spite of the otherwise clear weather [*Rey*, 1982].

2. Experiment and methodology

The following chapter describes the choice and processing of data and statistical parameters. It also describes the method used to calculate and present trajectories.

The presented work is an attempt to characterize the aerosol in Arctic during one year. Airborne particles were measured at the baseline station at Ny-Ålesund, Svalbard, between March 2000 and April 2001. Two instruments were used, a Condensation Particle Counter (CPC) and a Differential Mobility Particle Sizer (DMPS). The DMPS instrument measured particles with size diameter between 0.02-0.631 μm.

2.1 Instruments and tools

The station on Zeppelin Mountain, located 474 m a.s.l, was officially opened in 1990 (it was re-opened in May 2000) and is part of the "Ny-Ålesund International Arctic Research and Monitoring Facility". The Zeppelin Station for Air Monitoring and Research is owned and operated by the Norwegian Polar Institute. The Norwegian Institute for Air Research (NILU) is responsible for the scientific programmes at the station, including the coordination of the scientific activities undertaken by NILU and other institutions, as well as a number of international research groups´ campaigns. Department of Meteorology at Stockholm University (MISU) is present on Zeppelin Mountain and co-operates closely with NILU in developing the scientific activities and programmes at the station. In a collaborative effort, ITM operates a Condensation Particle Counters (CPC) and a Differential Mobility Particle Sizer (DMPS), [Internet 5].

2.1.1 CPC-Condensation Particle Counter

The ability of minute particles to grow to micrometer-sized droplets in a supersaturated environment can be exploited to measure their number concentration. Instruments that do this are called Condensation Particle Counter (CPC). These instruments let a small aerosol particle pass through an environment saturated by alcohol vapour and then quickly cool the vapour creating a supersaturation and causing the aerosol to grow by condensation. The aerosol particle grows to a size of about 10μm in diameter, which readily can be detected by an optical method. A schematic of the instrument principle is presented in figure 6.

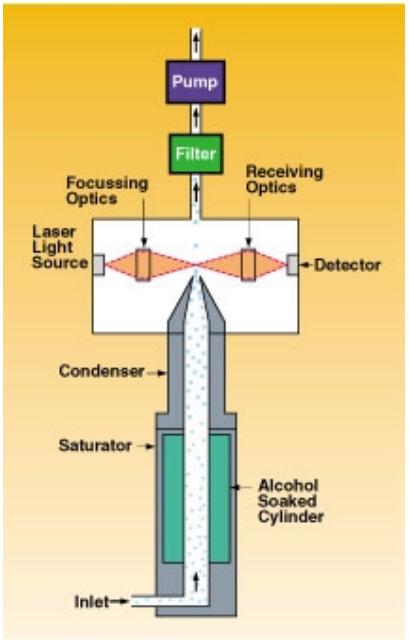

Fig. 6. Schematic picture of a CPC, [Internet 6].

To start with, the aerosol sample enters a chamber with supersaturated alcohol vapour. When the vapour surrounding the particles reaches a certain degree of supersaturation, the vapour begins to condense onto the particles, causing them to grow into larger droplets. The degree of supersaturation is measured as a saturation ratio (P/Ps), which is defined as the actual vapour partial pressure divided by the saturation vapour pressure for a given temperature. The lower size sensitivity of the counter is

determined by the operating saturation ratio. For the CPC this ratio is several hundred percent, whereas in the atmosphere, this ratio rarely exceeds a few percent for water.

Subsequently the enlarged particles pass from the condenser tube through a nozzle into the optical detector. The sensor's focusing optic consists of a laser diode, collimating lens, and cylindrical lens. This combination forms a horizontal ribbon of laser light above the aerosol exit nozzle. The collecting optics incorporate a pair of aspheric lenses that collect forward scattered light onto a low-noise photodiode. The signals from the photodiode are evaluated by a microprocessor. The microprocessor utilizes built-in analogue to digital converters to monitor temperatures, voltages, and pressure drop of the CPC. It is a counter within the microprocessor that keeps track of the particle pulses detected by the photodetector. The display, pushbutton, and RS2332 communications are also controlled by the microprocessor.

2.1.2 DMPS – Differential Mobility Particle Sizer

The particle size distribution measurement was performed by a Differential Mobility Particle Sizer (DMPS). The system consists of three main elements, a neutralizer, a Differential Mobility Analyser (DMA), and a CPC. A narrow size range of particles is selected by means of electrical mobility and counted by a CPC. By stepping trough the different mobilities an aerosol size distribution can be derived.

Before the distribution can be measured, the aerosols have to reach charge equilibrium. A small radioactive source neutralizes the aerosol particles by producing equal number of positively and negatively charged particles according to a known distribution as function of particle size. Given sufficient residence time in the neutralizer, the charge level on the aerosol particles is reduced to the Fuchs equilibrium condition.

Subsequently the sample enters a DMA, fig 7. The DMA consists of two concentric cylindrical electrodes. A negative high voltage is applied to the centre electrode; the outer electrode is at ground potential. An inner core of particle free sheath air and an outer annular ring of the aerosol sample flow down between the electrodes. The flow is laminar without any macroscopic mixing processes between sheath air and aerosol sample flow. Positively charged particles are attracted through the sheath air to the inner electrode. The pathway of a particle is a function the flow-rate, the DMA geometry, the applied voltage (electric field), the particle diameter and the number of elementary charges on the particle. Particles of a narrow and well-defined mobility range meet a narrow slit at the bottom of the centre electrode and are directed to further examination equipment. The positively charged particles of the other mobilities pass the exhaust outlet port without any further interest.

At the end of this system a part of the sample is introduced into a Condensation Particle Counter as described above. The lower size limit and maximum and minimum concentrations that can be measured are determined by the capabilities of the CPC that is used. Stepping or continuously scanning through the voltage range can obtain the entire submicrometer particle size distribution.

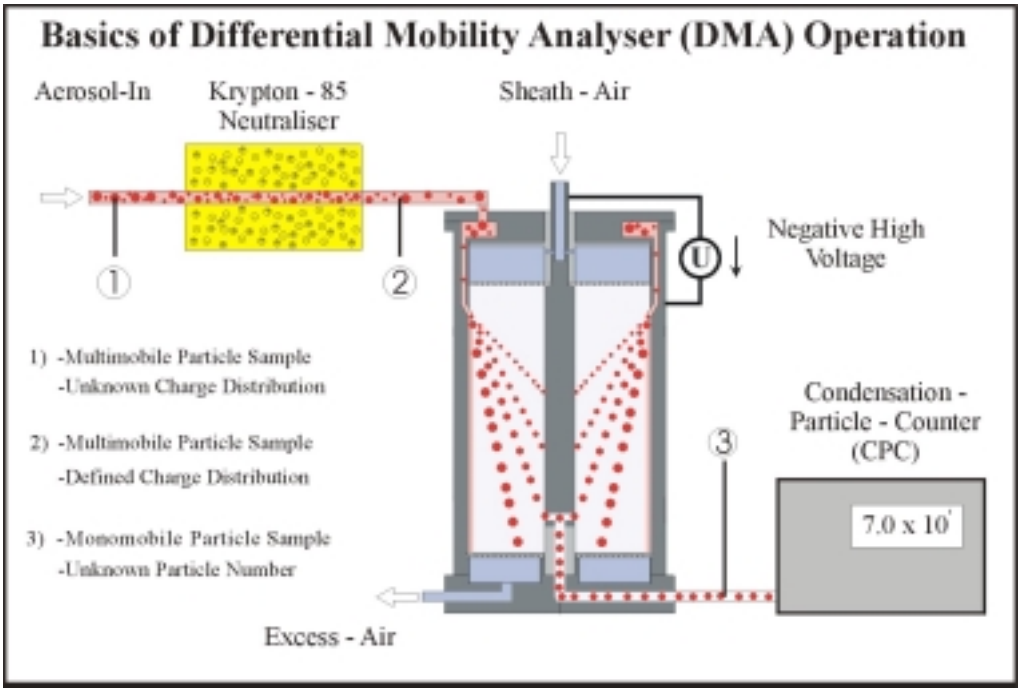

Fig. 7. Differential Mobility Particle Sizer (DMPS), [Internet 6].

2.1.3 Hysplit Description

To calculate an air parcels travel route and dispersion, different models that include meteorological data can be used. Basically, the model calculates the parcels trajectory, which is the curve in space that tracing the points successively occupied by the particle in motion. There are quite a wide variety of models available for modeling of long-range transport over regional and trans-boundary scales

The HYSPLIT (HYbrid Single-Particle Lagrangian Integrated Trajectory) model is a complete web-aplication for computing simple air parcel trajectories to complex dispersion and deposition simulations. The model is a result of a joint effort between NOAA and Australia's Bureau of Meteorology, and it has recently been upgraded. New features include improved advection algorithms, updated stability and dispersion equations, a new graphical user interface and the option to include modules for chemical transformations. Without the additional dispersion modules, HYSPLIT computes the advection of a single pollutant particle, or simply its trajectory.

The dispersion of aerosols is calculated by assuming either puff or particle dispersion. In the puff model, puffs expand until they exceed the size of the meteorological grid cell (either horizontally or vertically) and then split into several new puffs, each with it's share of the pollutant mass. In the particle model, a fixed number of initial particles are advected about the model domain by the mean wind field and a turbulent component. The model's default configuration assumes a puff distribution in the horizontal and particle dispersion in the vertical direction. In this way, the greater accuracy of the vertical dispersion parameterization of the particle model is combined with the advantage of having an ever-expanding number of particles represent the distribution, [Internet 7].

A trajectory is the time integration of the position of a parcel of air as it is transported by the wind. The parcel's passive transport by the wind is computed from the average of the three-dimensional velocity vectors at the particle's initial-position P(t) and its first-guess position P'(t+dt). The velocity vectors are interpolated in both space and time.

The first guess position is

$$P'(t+dt) = P(t) + V(P,t)\, dt, \qquad (5)$$

and the final position is

$$P(t+dt) = P(t) + 0.5\, [\, V(P,t) + V(P',t+dt)\,]\, dt \qquad (6)$$

2.2 Preprocessing

To investigate the relationship among total concentration, particle size and time of the year, different parameters have been chosen and calculated. The calculations were done using the calculation programs Excel (version 2000) from Microsoft Co. and Microcal Origin 6.0 (2).

The data sets were corrected to reduce errors in the result. Values showing –999 and 0 were subsequently deleted. These values were obviously errors, most likely because of data interruption caused when servicing the instruments or power breakdowns.

2.2.1 DMPS

The measurements from the Differential Mobility Particle Sizer were used in order to investigate the physical properties of the Arctic aerosol. To obtain an estimation of the different parameters, aerosol size distributions measured for three hours periods were examined. To start with, the size distribution was acquired every second minute, but later the result was reduced in time to make it easier to work with. A three-hour mean was selected to represent the measurements.

In order to investigate seasonal variations, the total aerosol number concentration has been calculated for the measured number size distribution by integrating the size distribution ranging from 0.02 μm to 0.631 μm.

$$N_{tot} = \int dN/d\log Dp * d\log Dp = \int dN \qquad (cm^{-3}) \qquad (7)$$

Where: N_{tot}=Total number concentration

The surface and volume of total particles were calculated to find out if there are any seasonal variation in the aerosol surface area and volume. These calculations tell us about the properties of the size distribution, with a large surface and volume indicating a large number of bigger particles. The surface is calculated for every size and then added together to receive a total value.

$$S_{tot} = \int dS * Ntot \qquad (\mu m^2\ cm^{-3}) \qquad (8)$$

$$S=d^2*\pi*/4*C \quad (9)$$

Where: S_{tot}=Total surface area
S=Surface area
C=concentration
d=diameter

Volume is treated analogous to surface.

$$V_{tot}=\int dV*Ntot \quad (\mu m^3\ cm^{-3}) \quad (10)$$

$$V=\pi*d^3/6*C$$

Where: V_{tot}=total volume
V=Volume
d=diameter
C=concentration

The effective diameter is calculated through dividing the volume with the surface, so that the relation between small and big particles is received. This will show the share of small particles compared to big ones. If Deff is low, the fraction of small particles dominates.

$$Deff=sum(nd^3*nd^2) \quad (\mu m) \quad (11)$$

Where: Deff=volume / surface

Another way to find out relations between particle sizes is to divide small particle number concentration by large particle number concentration. This tells us about the gradient between the two selected size classes. In this case, the sum of the three smallest size classes number concentration, (0.02, 0.0251, 0.0316μm) are divided with the sum of the following four size classes number concentration (0.0398, 0.0501, 0.0631, 0.0794μm). We termed this ratio δ. Hence, δ_1 is given by,

$$\delta_1=N_{20\text{-}32} / N_{40\text{-}79} \quad (12)$$

Where: δ_1= Relation between small particles and big particles for given sizes.
$N_{20\text{-}32}$= Total number concentration for the sizes 0.02, 0.0251 and 0.0316μm.
$N_{40\text{-}79}$= Total number concentration for the sizes 0.0398, 0.0501, 0.0631 and 0.0794μm.

2.2.2 CPC

The measurements from the CPC instrument have been used to calculate the frequency distribution of the particle concentration among some predefined size intervals. To obtain such a frequency distribution, a range interval of 50 concentration bins was defined, resulting

in 146 bins. To get the seasonal variation, every 14 months was evaluated, from Mars 2000 to April 2001. The figures were then plotted in a logarithmic scale.

2.2.3 Trajectory selection

Ten days back trajectories for air parcels arriving at 500 meters above sea level (because of the height of Zeppelin Mountain) for all selected cases were calculated to trace the history of the sampled air masses. This is done by means of tracking the origin of air with help of backward trajectories starting at Svalbard, and addressing typical patterns of the air mass measured at the receptor to the source area. Some 20 to 27 trajectories in nine different groups of parameters, as seen in table 1, were calculated with help of the HYSPLIT model provided by NOAA, [Internet 7].

Ending time and date for each trajectory was selected from earlier described histogram for each parameter; number, size relations, surface, and volume. In some groups criteria are based on typical events that characterize the period. In other groups more odd events are of interest and therefore chosen to see if the result differ from normal situations. It is especially interesting to specify conditions when either small particles dominates the size distribution or when big particles are enriched. Since younger aerosol particles are generally smaller, the particle size distribution can indicate whether the aerosol was produced locally or more far away from the measurement point. Criteria for different groups are shown in table 1, for exact dates see appendix 1.

Table 1. The trajectories are selected based on different criteria. The table describes these criteria for every parameter.

Parameter	Criteria	Description	Time period of occurrence	Number of events
N	>1000	Particle concentration higher than 1000 cm^{-3}	Mars-Oct.	23
δ	>3	This parameter is constructed by dividing the sum of the particle concentration found in the first three bin sizes with the sum of the aerosol concentration observed in 4 subsequent bin sizes. This ration gives a number describing the steepness of the slope. Higher value than 3.	May-dec.	27
Deff	<0.11	Also here a high fraction of small particles is seeking, an effective diameter less than 0.11.	May-Oct	23
Deff	>0.19	A high Deff show that the fraction of big particles is high, in these cases higher than 0.19	Oct.-May	23
Deff	>0.15	During the summer Deff average is low, but in some cases it rises. These cases, with a Deff higher than 0.15, are pointed out in this group	June-Sep	23
S	>10	Situations with surface larger than 10 μm^2 cm^{-3}	Mars-May	20
S	<1	Cases with a smaller surface than 1 μm^2 cm^{-3}	June-Oct	20

V	> 0.5	The criteria here are a volume value higher than 0.5 $\mu m^3 cm^{-3}$	Aug.-May	20
V	< 0.1	Smaller volume than 0.1 $\mu m^3 cm^{-3}$ indicates cases with low volume	May-Oct	20

In order to address the typical criteria set up above to source patterns of the air-masses, a new grid system is set up with the north pole moved to 79 N 12 E, the location of the measuring station. The grid system is divided in 20 sectors (18° latitude each) and each latitudinal sector is then subdivided in cells separated by 2.5° longitudes. For each situation of interest, the trajectories is investigated in order to find out what cells in the grid system the air-mass has crossed before arriving to the receptor site. Doing this for the total number of trajectories fulfilling the criteria, and plotting the frequency of air masses residing in each and every cell, the result is a color-coded description of the preferred pathways for the air masses showing the characteristic property. This is a useful tool to obtain information about the air-mass history in terms of geographical source locations for the specific air masses having the different aerosol properties.

3. Results

The results of the measurements and calculations of statistical parameters and trajectories are described in this chapter. The relationships between different parameters are presented as well as its relation to time of the year. Finally the result of the trajectory analysis and the distribution of aerosols are presented.

3.1 DMPS

3.1.1. Particle Number Concentration

Three-hour average particle concentrations covering one-year data from Spitsbergen are presented in fig 8. In the Arctic the aerosol concentration show pronounced seasonal variation, with a maximum from June to August, i.e. Arctic summer, and a minimum in winter, November to March.

The difference between winter and summer month is many times as high as thousands of particles. In winter, the concentrations were generally low. It appears distinctly that the aerosol number concentration drops around Julian day of 300 (26th of October) and continues to stay low until the end of February. The variation between episodes with high and low number concentrations is a lot bigger in summer than in winter. In winter there are hardly any visible variations in aerosol number density. In the beginning of March (day 60-75) some data are missing, but it is expected that it should follow the trend.

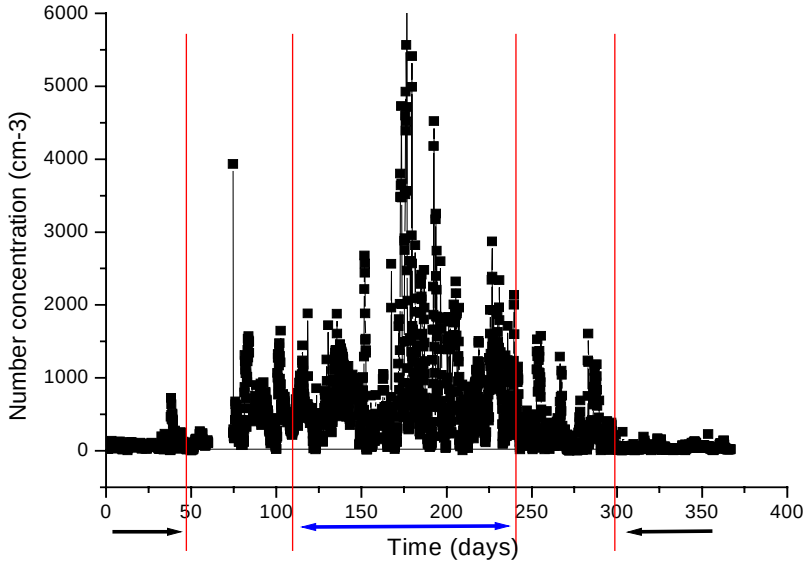

Fig. 8. The total aerosol number concentration for the period from March 2000 to March 2001. The maximum number concentration is in summer (day 150-240) and the minimum in winter (around day 300 to 75). Arrows at the extreme, indicates days of polar night and the double-headed arrow in the middle indicates days of midnight sun.

3.1.2. Volume and Surface

The calculated aerosol volume reaches highest values in spring, from Mars through May (day 75 to 149) as shown in fig 9. During the summer season the aerosol volume was generally smaller compared to spring. The lowest aerosol volume was observed during the polar night, with values under 0.05μm^3 cm^{-3}, expatiated a short rise in February.

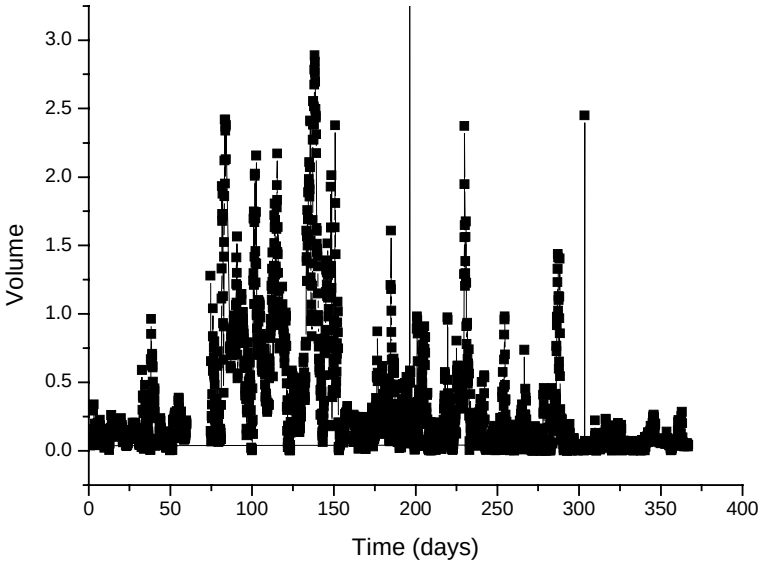

Fig 9. The aerosol volume (μm^3 cm^{-3}) distribution for the period March 2000 to March 2001. The maximum can be found in springtime (around day 50 to day 149) and the minimum in winter (around day 300 to day 75).

Calculated aerosol surface and volume show a similar evolution over the measurement period, (fig. 9 and 10). Highest values are observed in spring with values as high as 23μm^2 cm^{-3}. The summer and autumn has a smaller aerosol surface compared to spring, as shown in fig 10. In winter the surfaces is even smaller, it never reaches the same level as the rest of the year. Only one period during winter show a surface value higher than 6μm^2 cm^{-3}, which is around day 75 in the middle of March.

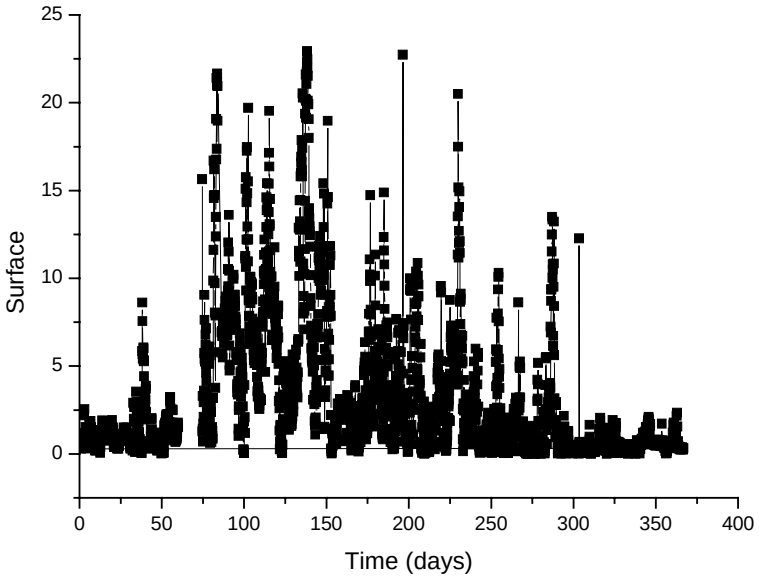

Fig 10. The observed aerosol surface (μm^2 cm^{-3}) for the period March 2000 to March 2001. There are a lot higher values in spring, around day 50 to day 150, than the rest of the year.

3.1.3. Size relations

Relations among different particle sizes show the same seasonal pattern as the parameters presented above. The result in fig. 11 tells something about the influence of small particle. From June to October Deff is generally low, under 0.15µm, which means that there are a higher fraction of small particles that time a year compared to the rest of the year. There is one period during the year, between day 300 and day 50 (winter), when the Deff value exceeds 0.2µm. During that period the larger particles were more abundant than during the rest of the year.

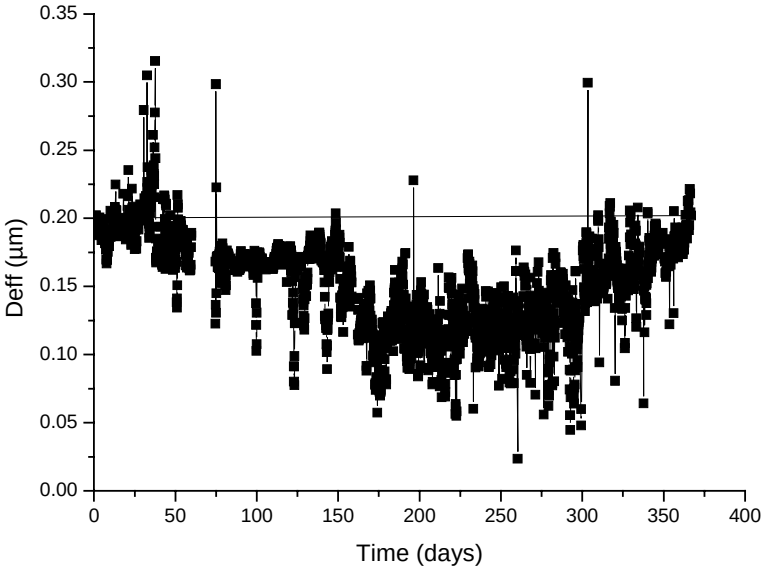

Fig 11. The effective diameter (Deff) for the year has a minimum during the summer and a maximum during the winter.

The result for the calculated δ is shown in figure 12. When δ is larger than 1, particles below 0.0316µm dominates. This is typical for the warmer period from May to October (day 125 to day 300). During the winter period, on the other hand, particles in the upper size range (0.0398, 0.0501, 0.0631, 0.0794µm) dominate. This is especially true for November, when δ is very low. A high δ is an indicative of a recent formation of new particles.

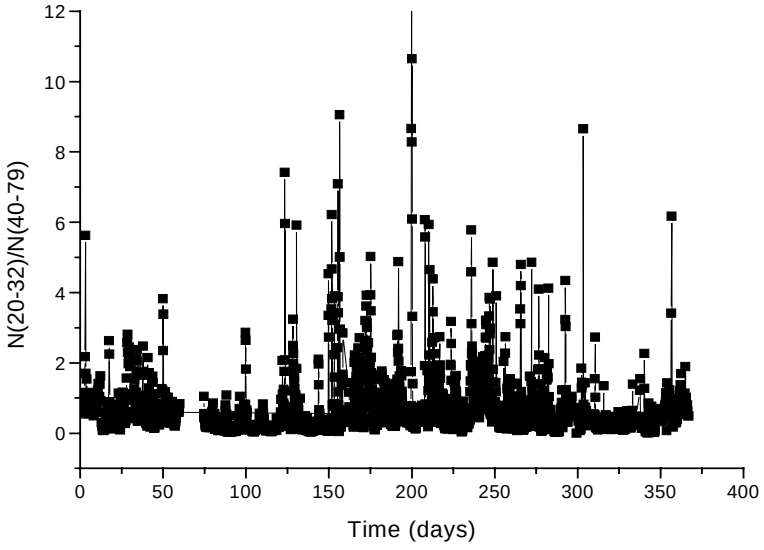

Fig. 12. The diagram for δ calculation, with time in days on x-axis and δ on y-axis. The figure shows a bit lower values for November (day 300 to 330) than for the rest of the year.

3.2 CPC

To investigate the seasonal variation of episodes with high or low total aerosol concentrations, monthly frequency distributions of the observed aerosol number densities are shown in figures 14-27. Clear differences between different months and different seasons were observed. From September to April the aerosol number concentration are most of the times below 1000cm^{-3}. The frequency distributions of the observed aerosol number densities are similar for the months from October to January (figure 15 and 16). This means that we have many occasions with low particle number concentration during winter, but almost never occasions with high total number concentration. In May the frequency for higher aerosol number concentrations raises and stays high in June, July and August as well (fig. 13 and 14). The summer has thereby very often a high aerosol number concentration of particles, sometimes higher than 5000 cm^{-3}. Even if the frequency of high number concentration occurs often during summer, there are also many occasions with low number concentration. The change between one season and the following season are quite obvious. For instance, in August episodes with aerosol number concentrations higher than 2000cm^{-3} is common, however in September such episodes become rare. The difference between April and May is also very clear, with a much higher frequency of large aerosol number concentration in May (fig. 13). A comparison between Mars and April year 2000 and Mars and April year 2001 did not show any large difference (fig. 13 and 17).

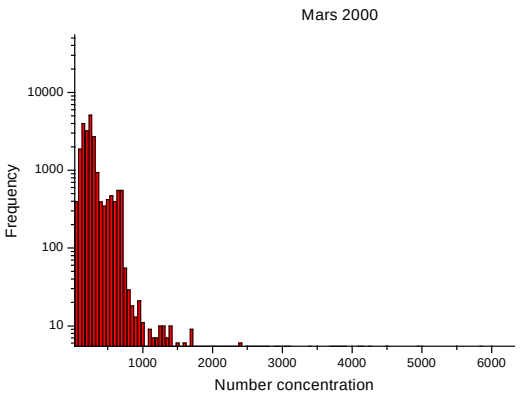

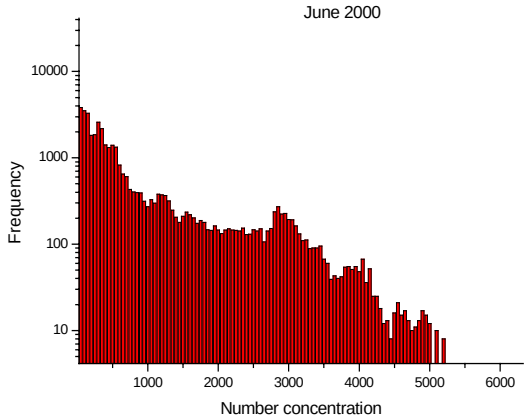

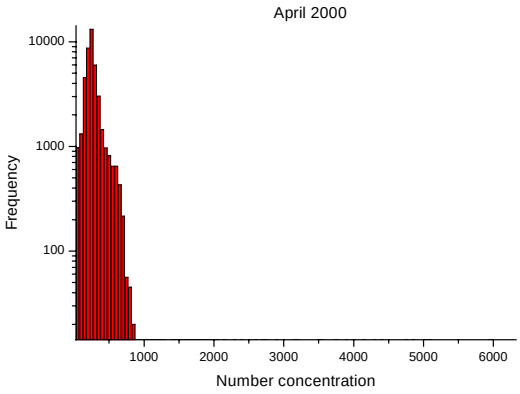

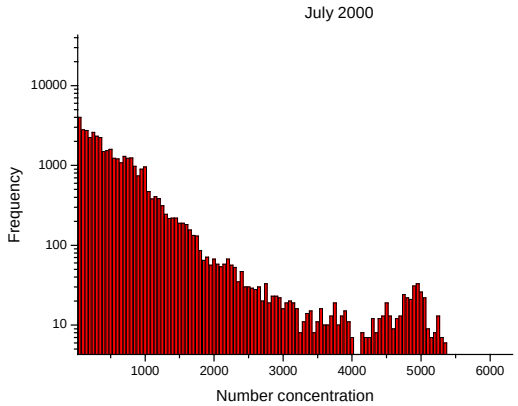

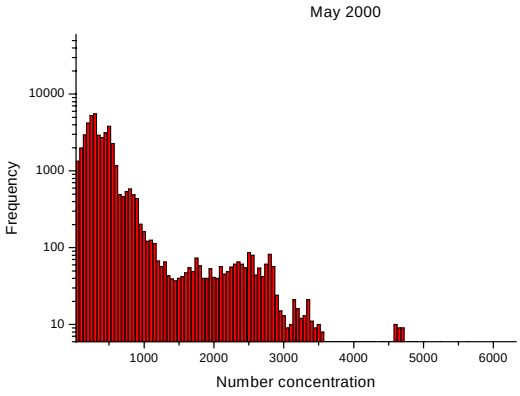

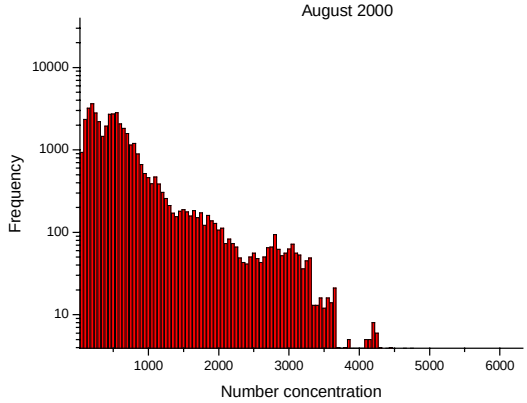

Fig. 13. Frequency of observations for spring 2000, March, April and May. In May the frequency for higher number concentrations (cm^{-3}) are a lot higher than for March and April.

Fig. 14. Histograms of the frequency of observations for summer 2000, June, July and August. X-axis show number concentration in cm^{-3}.

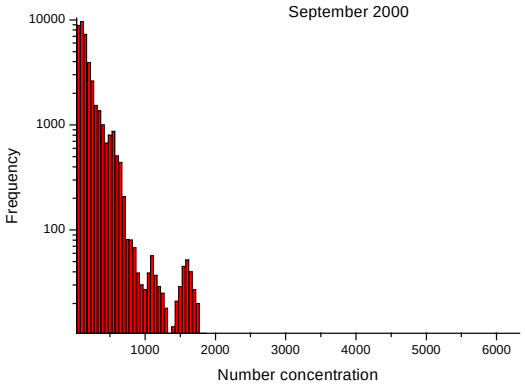

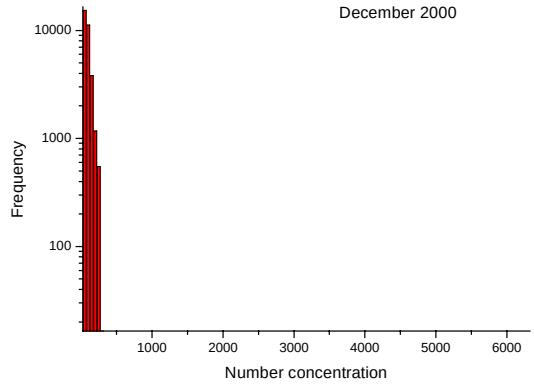

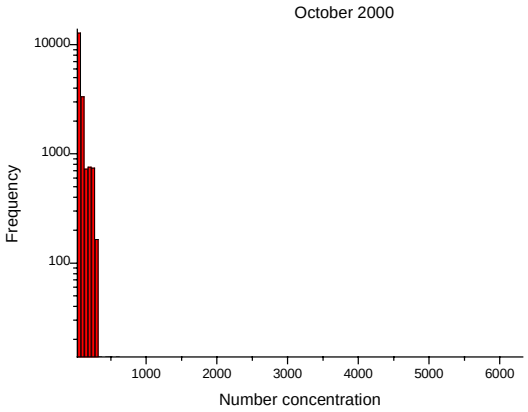

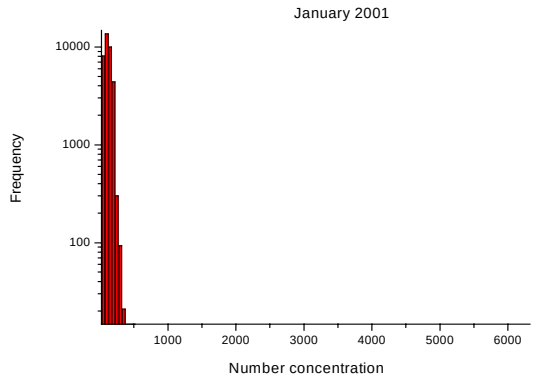

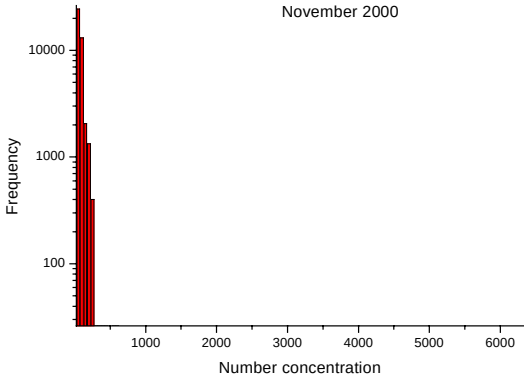

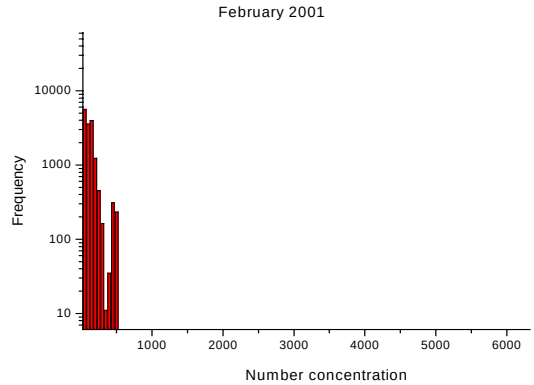

Fig. 15. Frequency of observations for September, October and November 2000. X-axis show number concentration in cm^{-3}.

Fig. 16. Histograms of frequency of observations for December 2000, January and February 2001. X-axis show number concentration in cm^{-3}.

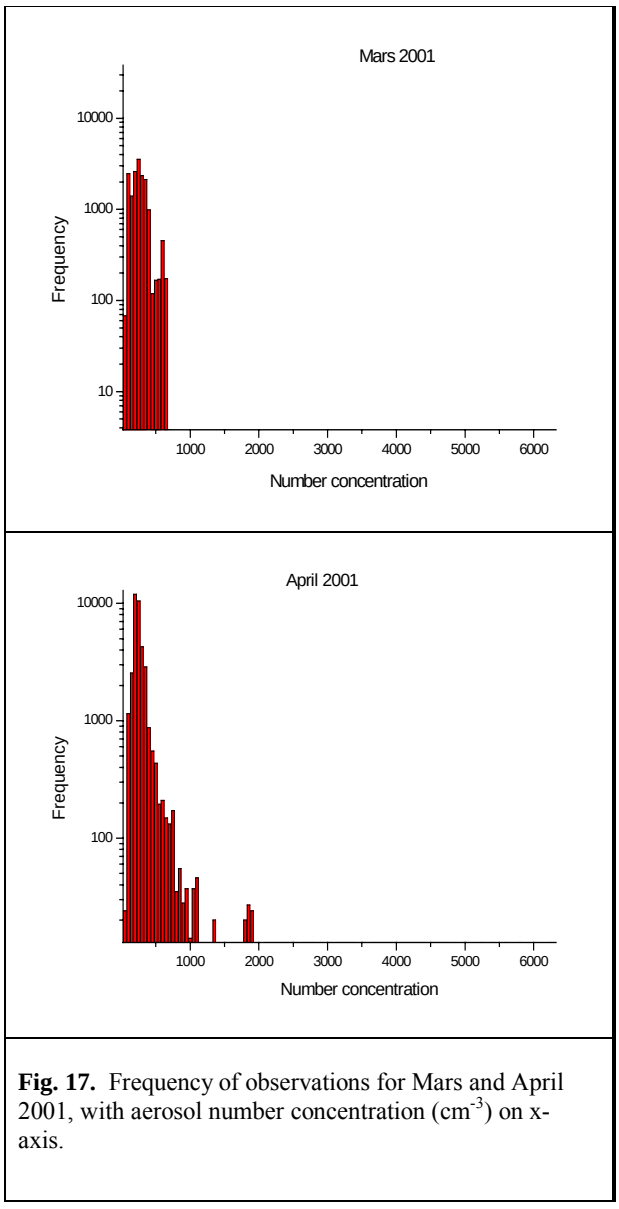

Fig. 17. Frequency of observations for Mars and April 2001, with aerosol number concentration (cm^{-3}) on x-axis.

3.3 Trajectory

Figures 18-26 show the result from the trajectory calculations.

The plot generated from trajectories selected from periods when the total number concentration exceeded $400cm^{-3}$ shows few significant features. It can be seen in figure 18 that close to Svalbard the most favored direction is air arriving from the west. Away from the Svalbard there is a suggestion for air arriving from the Canadian Arctic. However, the probability is fairly low. Grid cells with more than 10 trajectories passing through the area are rare.

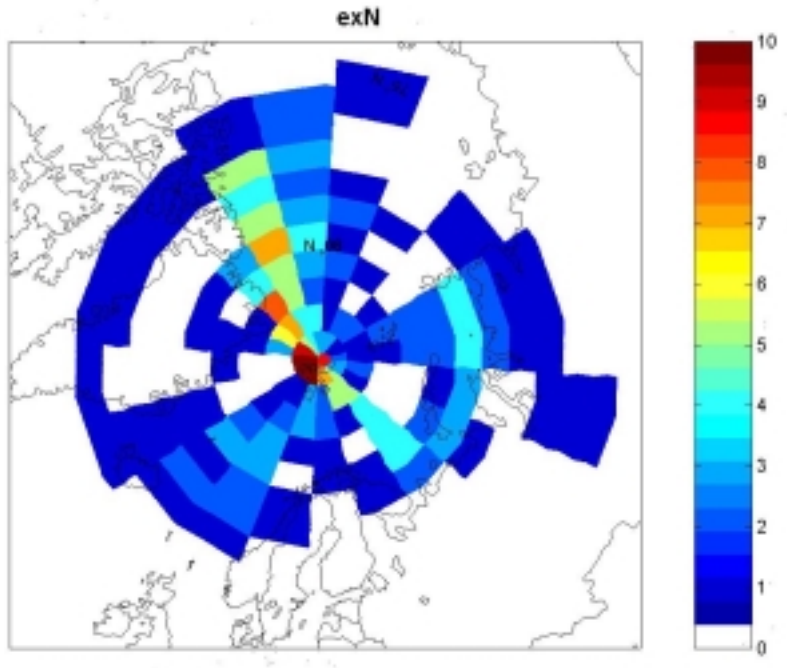

Fig. 18. Plot of trajectories from total number concentration group (>400cm^{-3}). It represents possible source areas for air masses with high number concentration of aerosols. The colours represent number of trajectories passing through the cell.

The largest probability for δ trajectories is shown for trajectories arriving from the Fram Strait between Greenland and Svalbard, as can be seen in figure 19. The sector between 30 and 130 degrees present the lowest probability. This is similar as to what is found for the previous criteria using the total number as a threshold.

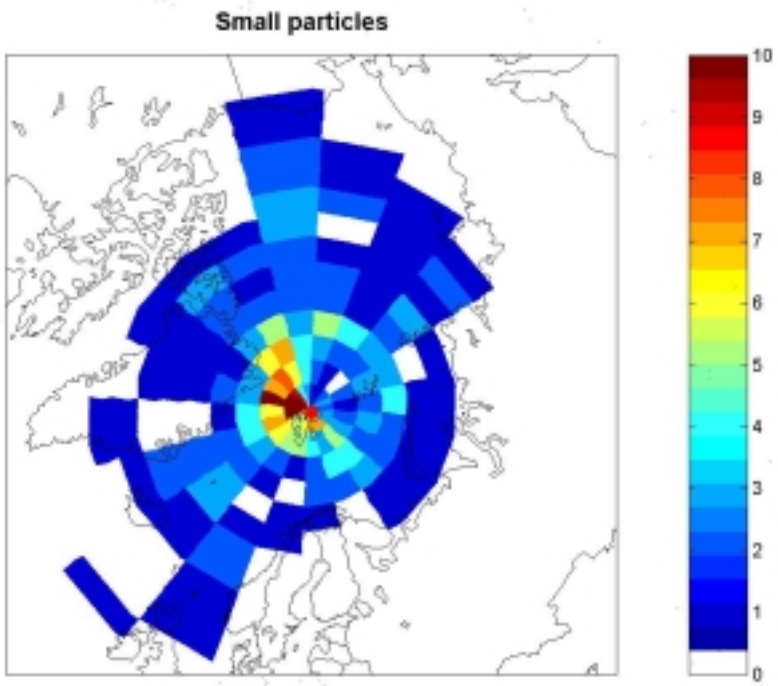

Fig. 19. Trajectories plot from δ factor. The colours represent number of trajectories passing through the cell.

Three threshold values were used for the effective diameter. Episodes when we observed enhanced particles are characterized by a Deff value higher than 0.19μm, whereas small particles are characterized by a Deff value lower than 0.11μm. The differences in air mass origin for these both cases can be seen on Fig. 20 and 21. Clearly the two plots are different. The trajectory pattern for the cases with Deff smaller than 0.11 μm suggests a branch stretching towards the Canadian Arctic north of Greenland. This is similar to the transport pattern shown in figure 19, but in case of Deff the described pathway is somehow clearer. The East is clearly the least probable sector for the small Deff criteria.

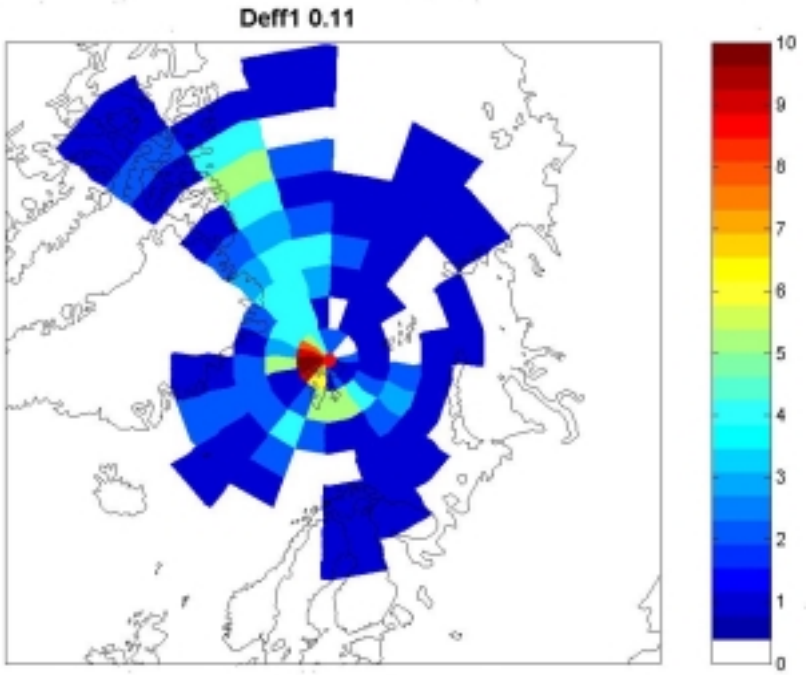

Fig. 20. Probability of the trajectory pathway for the observations with Deff factor less than 0.11µm. The colours represent number of trajectories passing through the cell.

As can be seen in figure 21, large Deff values are essentially associated with trajectories with an origin from the east or southeast. This is in direct contrast to the observations with small Deff values. Close to Svalbard more or less all directions are represented for the large Deff values.

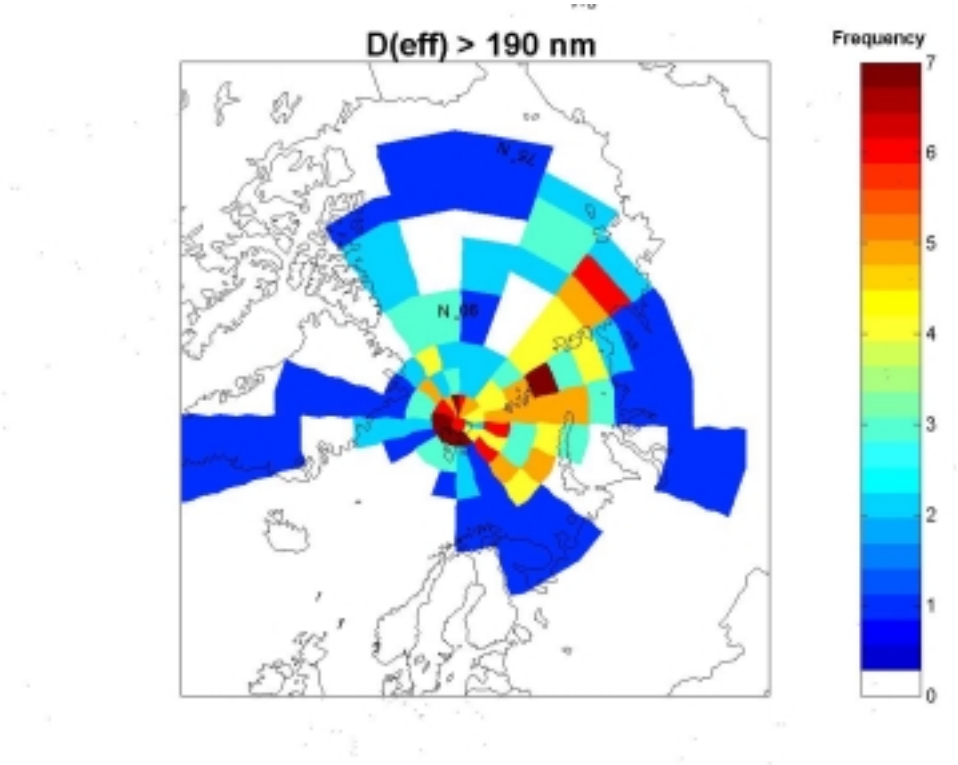

Fig. 21. Possible source regions for the air masses with a large fraction of large particles. The Deff value is higher than 0,19µm. The colours represent number of trajectories passing through the cell.

The third plot for the effective diameter show episodes during summer with a Deff value higher than 0.15µm (figure 22). The sector with the highest probability of the trajectory passing through lies between 160 and 300 degrees. Clearly air masses containing large particles arrive from Atlantic during summertime.

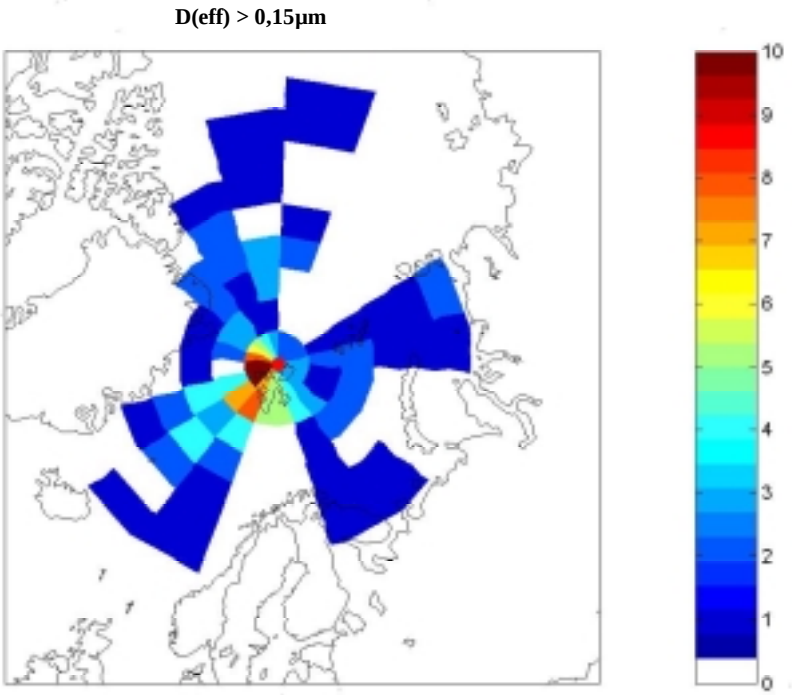

Fig. 22. Trajectory probability plot for the observations with a Deff higher than 0,15µm for summer months. The colours represent number of trajectories passing through the cell.

The plots, shown in fig. 23 and 24 are presenting transport pathways for two groups of data. The observations were divided using the aerosol surface as the key sorting parameter, giving one group with high aerosol surface and one with low aerosol surface. The characteristic features for the high and low aerosol surface are not as distinguishable as in the case of the high or low Deff. The plots picture a high north, northwest frequency, although the first case has a higher easterly frequency. The second case shows some southwest trajectories.

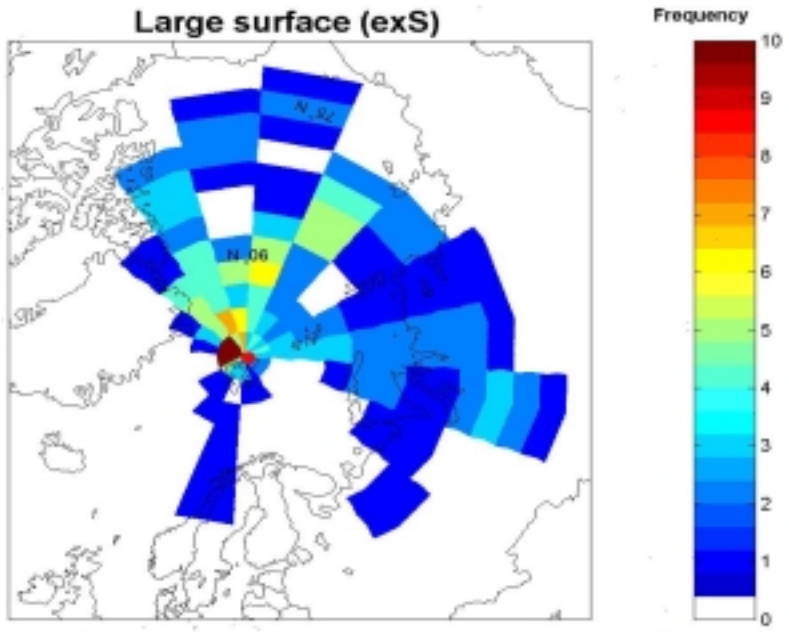

Fig. 23. Trajectories plot for the large surface criteria in spring. The colours represent number of trajectories passing through the cell.

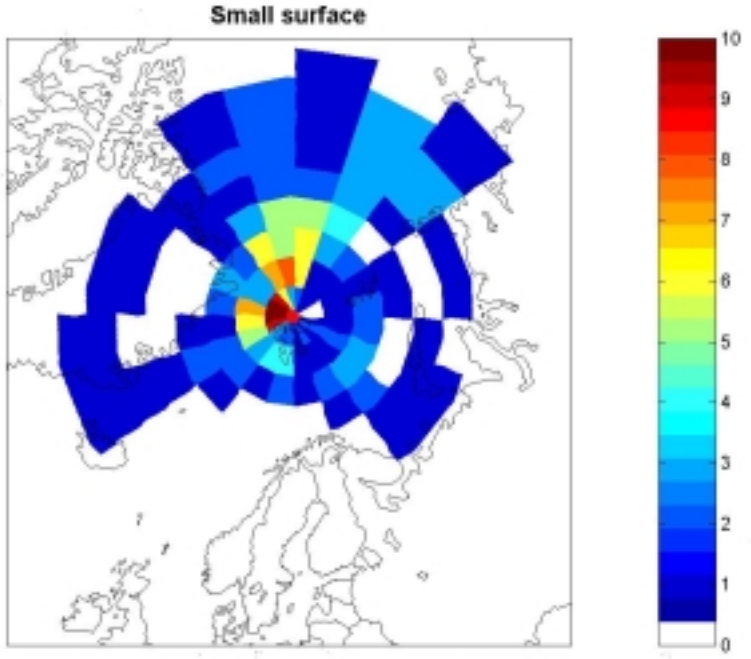

Fig. 24. Trajectories plot for the small surface criteria. The colours represent number of trajectories passing through the cell.

There are two plots using the aerosol volume as a critical factor (figure 25-26). The plot from the small aerosol volume as criteria was found to show almost the same picture as the surface plots; a little higher probability of air mass arriving to the Svalbard from the north-west direction (figure 26). In cases of the large aerosol volume (figure 25), the air masses seem to come from the directions between northwest and south, but close to Spitsbergen from other directions as well.

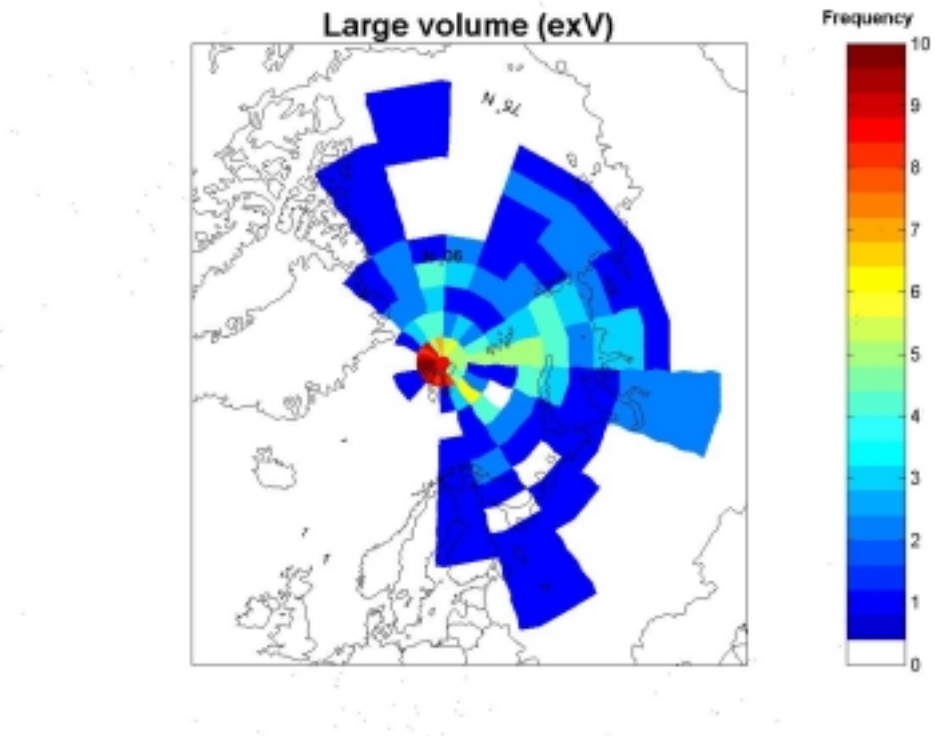

Fig. 25. Possible source regions for air masses with a large aerosol volume.

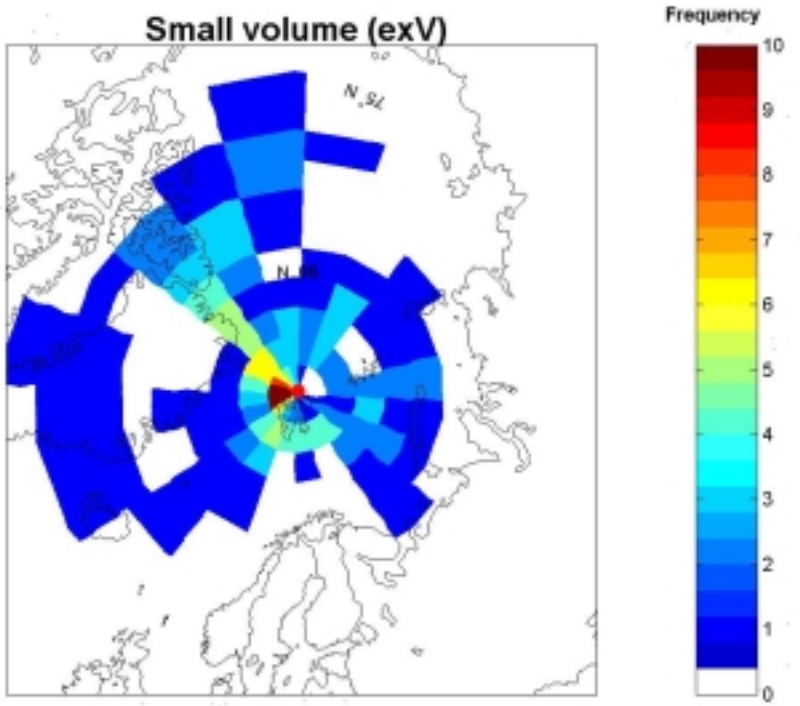

Fig. 26. Possible sources and preferred pathways for air masses with a small aerosol volume. The colours represent number of trajectories passing through the cell.

In general, the areas identified as having a high potential for situations with a larger fraction of large particles and, with high aerosol volume and surface lie in an easterly direction, and are mostly true for winter situations. Cases with air masses characterized by large aerosol surface show also a strong northerly component. The episodes when larger particles are high-represented summertime, on the other hand, the origin of the air masses is in southwest. Cases with a higher concentration of small particles, mostly summertime, can often be tracked backwards in a westerly direction. Closer to Svalbard all directions are represented.

4. Discussion

This chapter includes a discussion about how the Arctic aerosols are influenced of its origin. The result of the comparisons between different parameters and time of the year are also discussed.

4.1 Aerosol Number Concentration and Size Distributions

The results clearly show an unambiguous variation in the number concentration of the Arctic aerosol depending on season. The aerosol number concentration has a summer maximum and a winter minimum. This is the opposite of many other studies who often show a very clean atmosphere in the Arctic summer [*Carlson*, 1981] [*Xie et al.*, 1999a]. The picture of a clean Arctic summer is partly based on the absence of Arctic haze this time a year and the removal of particle mass in the summer. In this study particles in the size range from 0.02μm to 0.631μm were measured and evaluated. The particles within this size range covers particles

measured in Arctic haze layers, but smaller particles as well. The high result of aerosol number concentration during summer may partly be due to the smaller size range that is measured.

While the aerosol number concentration show a maximum in summer, the aerosol volume and surface show a maximum in spring. Though the total number concentration also shows higher values in spring, but not in the same extent, the particles are not only getting more numerous, but larger as well this time. In the middle of March the aerosol volume and surface calculations indicate a slightly higher values compared to the rest of the month. This could maybe be a sign of an episode of Arctic haze. The reason for the seasonal variation of the Arctic aerosol can mainly be explained by **the atmospheric circulation, differences in removal processes, and the sunlight.**

It is clear that the aerosol number concentration show a relation to the presence of sunlight. When the sun is present, the photochemical aerosol production contributes to the total aerosol number concentration. On the other hand, the new particle formation is very low during the long polar night. As the sunlight moves northward in the spring, more photochemical reactions can occur, including photochemical conversion of SO_2 to acidic sulfate and production of particulate bromide and iodine. This can be the reason why the number of small particles gets higher. The aerosol number concentration is also getting higher as the days are getting longer.

Rahn's coupling/decoupling hypothesis gives us another explanation to the seasonal variation of the aerosols. In winter the polar front is situated south of many sources in Eurasia and America. At the end of the winter, the air masses stretch from North America to Eurasia where they pick up pollutants. At the beginning of spring the polar front favors transport towards high latitudes bringing the pollutants into the Arctic. The aerosols are then removed from the atmosphere by cloud condensation followed by precipitation. This could explain the high volume and surface values in spring, followed by a drop in summer. Also, in the summer, the polar front is situated north of the continental sources. As result, pollutions are not given the same chance to reach the Arctic as in winter. If the air has low number concentration of pre-existing particles, in this case summertime, new particle formation occurs frequently, giving many small particles as result. The absence of large particles also eliminates for condensation to occur, since large particles act as a sink for condensable gases and small particles. Therefore the particles in the clean air summertime do not grow in size to the same extent as they do in unclean air.

The seasonal trend of the Deff and δ indicates that smaller particles are during summer relatively more abundant in comparison with larger particles. During winter, however, the situation is opposite. One reason to the smaller particles summertime is that the atmospheric removal processes are much more efficient and that precipitation occurs to a larger extent in summer than in winter. As a consequence, during summer a significant portion of the particles are washed out of the atmosphere. Thus the particles are not given enough time in order to grow to the same size as observed in winter. The conditions for new particle formation are improved after precipitation, due to fact that the atmosphere is not saturated, and this can lead to higher number concentrations of small particles. As mentioned earlier, precipitation activity is higher during summer and thus the enhanced fine aerosol number densities are also observed during the same part of the year. Since the removal processes are less intensive in winter, the aerosol residence time in the atmosphere becomes longer. As a result, the conditions for the growth of the particles by coagulation and condensation are better.

Another theory is that more local Arctic sources contribute to the biogenic aerosol through DMS oxidation. The DMS is of the oceanic origin and the role of DMS becomes more important as the sea ice melts in the early summer. The summer peak in aerosol number concentration is in that matter partly due to DMS from local Arctic Ocean. The contribution of the other high latitude parts of the oceans to the DMS in the atmosphere cannot be excluded.

The result from the CPC measurements show frequent occasions with low aerosol number concentration during winter and many occasions of high number concentration in summer. This result agrees with our pattern of the Arctic aerosol variation described earlier, with a maximum in particles number concentration in summer and a minimum in winter and is partly explained in the same way. One explanation is that the sun never rises above the horizon in winter, which eliminates for photochemical particles to be produced (see above). Rahn's coupling/decoupling hypothesis is another explanation. It can be seen clearly in the diagrams that the concentration drops noticeably in October, and at the same time the rate of big particles rises. The same occurs, but in the opposite direction, in spring both the number concentrations and the rate of small particles increase abruptly. Another reason is the differences in removal processes between summer and winter (see above). The comparison between March and April 2000 and March and April 2001 indicate that the data set is representative for the sampling site, since the observations for both periods are almost identical.

4.2 Air mass origin

The analysis of the backward trajectories provided information on the likely source locations or preferred aerosol transport pathways to Svalbard. The trajectories can tell us something about the long-range transport, even though there are several constrains with this kind of analyses. The cumulative error in the parcel location beyond 5 days of simulation becomes very large. In this study 10-day trajectories have been used. Even if the errors in trajectory calculations were probably large, we believe that useful information about the origin of the air masses observed at Svalbard still can be obtained. The error in a trajectory calculation is primarily due to the fact that meteorological fields, which vary continuously in space and time, are at times poorly represented by a field defined at fixed locations (grid resolution) and at fixed temporal intervals. The other error, more an error in interpretation than calculation, is that a particular trajectory may have little relationship to the air plume dispersion pattern. Trajectories only represent the flow path of a single particle at the time of the initial release. As an air mass spreads out both horizontally and vertically due to dispersion, it may take many different paths in addition to the initial trajectory. The air parcel may also change character by mixing with the surrounding air.

The trajectories from the total number concentration group show few significant features and almost every direction are represented. There is though a link between air arriving from west and from the Canadian Arctic and the observed high particle number concentrations. It is possibly that these air masses bring with it high load with emissions. Another explanation is that this may be the most favored wind direction throughout the year. As figure 5 suggests, the wind direction during wintertime is more common from north than from east. The trajectories are selected almost all around the year, and it is also possible that the number of trajectories is too few to find a clear pattern. It is also likely that the differences between seasons are so big that is not possible to mix them. Maybe the season is more important than

number concentration? There is no doubt that observations over the many years are needed in order to verify the observed patterns statistically.

The hypothesis about the trajectories from aerosol volume and surface groups was similar to the one presented for aerosol number concentration. Backward trajectories typical for cases when large aerosol volume was observed originated probably over Eurasia, however, the large aerosol surface was observed in air masses originated further north. The plots of small surface and volume are more similar with a pretty clear pattern from northwest.

Our trajectories from situations with a higher fraction of smaller particles are recorded mostly during summer. These trajectories indicate a more frequent westerly pattern. According to [*Xie et al.*, 1999b], more local/regional Arctic sources contribute to summer concentration, as our results confirm as well. One plot shows summer situations when the fraction of big particles dominates, which are not as common as the other way around. The picture is not in agreement with situations with higher fraction large particles selected from spring and fall. It is though possible that these air masses are influenced by long-range transport from Europe or that the previous period been dry.

Overall, long-range transport of aerosol is most probably more effective in winter than in summer. Air from continental sources, mainly from Europe and Russia, seems to contain large particles. Relatively high values of trajectories observed from Eurasia in winter could possibly be connected with the preferred pathways during the transport rather than with aerosol emissions in the Arctic. Thus, the major source of large particles in the Arctic during winter could be not a long-range transport itself, but SO_2 to SO_4^{2-} conversion during the transport. As particles are transported in the polluted air they grow, and their larger surface leads to higher fraction of the condensable species ending up on pre-existing particles.

4.3 Comparison with other studies

The study of long-range transport and seasonal variations of the Arctic aerosol presented here can be compared to at least three similar studies in the Arctic region. The first one deals with the ice-cores from Greenland at Dye 3 [*Lowenthal et al.*, 1997]. The second one includes data from the Alert, Canada [*Xie et al.*, 1999b] and the third study is based on data from Barrow, Alaska [*Polissar et al.*, 1999]. These studies are mostly focused on chemical compositions and seasonal variation of the sources, whereas in this study the aerosol properties related to long-range transport are the major objective. However, it is of interest to compare them anyway.

Pollisar et al. suggest that in winter and spring industrial regions in Eurasia and North America are the major sources of aerosol measured at Barrow. In summer they found that large areas of the North Pacific Ocean and the Arctic Ocean contribute to the observed high condensation nucleus condensations. Our results also show transport from Eurasia when we observed a high Deff value and a large aerosol volume and surface, which can be associated with higher fraction of large particles. Our plots for small particles (figure 15, 19 and 21), mainly associated with summer though we have a higher rate of small particles during summer, agree with Pollisar et al. who concludes that the summer maximum could be related to biogenic sulphur precursor emitted from the ocean. They summarize their study with saying that the long distance transport from industrial regions, photochemical aerosol production, emissions from biogenic activities in the ocean, and volcanic eruptions are major sources of the aerosol properties measured at Barrow.

Trace element concentrations and ratios were used by Lowenthal et al. to identify the continental origin of pollution aerosol at Dye 3, Greenland. The results show that both eastern North America and Europe contribute to the aerosol pollution observed. In general, air mass back trajectories for the Dye 3 samples were generally consistent with observed aerosol pollution chemistry. They also point out that during the month of April 1989, they indicated a persistent influence from European sources. While their back-trajectory analysis pointed to sources in the Arctic during this period, the chemistry of the aerosol showed that the ultimate source region must have been Europe. This is a good example of the meteorological complexity and the difficulties one might encounter when the air mass back trajectories are used to reproduce long transport. In such cases, the chemical fingerprint of the aerosol can be crucial for identifying the ultimate source area. In our study we have not studied the chemical compositions at all.

Airborne particulate samples were also collected at Alert, Canada, and later summarized by Xie et al.. They analyzed the chemical composition of the aerosols and also applied potential source contribution function analysis (PSCF). Chemistry is not detectable in our study of the number density of aerosols, but the potential sources can be compared anyway. Like our results, their study shows a strong seasonal variation in the Arctic aerosol. Anthropogenic aerosol represented by SO_4^{2-} and a number of metallic elements have a PSCF pattern with high values in the high emissions regions of Eurasia. It shows a concentration maximum starting from December and extending to February. As for particulate SO_4^{2-} transformed from SO_x, the PSCF pattern suggests the sources and origins in Europe, and the Asian part of Russia. It is in an agreement with our measurements. For the same period of the year we observed large aerosol volume and also high Deff. In the other words, larger aerosol particles were enhanced. The tundra areas in Alaska and NTW of Canada are the sources of soil dust observed at Alert. There are two maxima in the seasonal variation of soil factor, one in spring and another in the late summer period. Our high total number concentration throughout the year showed a weak north-westerly pattern as well as when we observed small particles summertime. The PSCF pattern of sea salt suggests that Atlantic Ocean is the main contributor and it has a broad contribution over the period from October to April. The high potential areas in their PSCF plot of biogenic aerosol source suggest that both low latitudinal Atlantic Ocean and local Arctic Ocean are the contributors of biogenic aerosol.

5. Summary and Conclusions

Aerosol data from Ny-Ålesund, Svalbard, for the period from Mars 2000 to April 2001 have been analyzed by different variables; total number concentration, surface, volume, the effective diameter and a ratio δ. The frequency of occasions over the year for the total number concentration is calculated as well. Meteorological information in the form of 10-day backward air parcel trajectories was used to locate the source origins and preferred transport pathway of Arctic aerosols.

Our analyses show a general trend for small and numerous particles to be associated with air from west, north-west. Periods when large particles strongly influence the aerosol population show a tendency of being associated with air from the east and north-east. This division can be linked to different periods of the year. The former dominate in summer and the latter in the winter. The calculated back trajectories show more clearly pattern of long-range transport in

winter than in summer. In summer large areas of the Arctic Ocean contribute to observed high number concentration and a higher rate of small particles.

Investigating the total number concentration we are able to classify the results according to season. Total number concentration has seasonal variations with its maximum in summer and minimum in winter. The effective diameter also shows a seasonal cycle with maximum in winter and minimum in summer. Nucleation events can explain the observed high aerosol number concentrations and the higher fraction of small particles during summer. The generally very stable polar night, the high load of pre-existing particles and the low precipitation wintertime might quench the nucleation due to condensation and coagulation, thereby the higher fraction of large particles that time a year. The particle volume and surface area has a maximum in spring.

It is clearly shown that the frequency distribution of the aerosol number concentrations in summer exceeds the one for winter. This means that in summer we observed many occasions of high number concentration, whereas in winter the occasions of low number concentration dominates.

Acknowledgement

I would like to express my gratitude to all personnel at the Institute of Applied Environmental Research, University of Stockholm. I'd like to thank my advisor Dr. Johan Ström for introducing me to this topic and for being available for questions, guidance and help and also for providing me with a large amount of literature.
I wish to thank Radovan Krejci and Birgitta Noone, for help with technical matter.
Most of all, Peter Tunved for having contributed with scientific knowledge and with invaluable help with the trajectorie plots.

Further on, I wish to thank Erik Kjellström, MISU for advises and linguistic issues with the text.

I wish to thank Karin Hall at the Department of Physical Geography, University of Lund for making this co-operation with ITM possible and for being my advisor in Lund.

References

Ahrens, C.D., *Meteorology Today*, West Publishing Company, New York, 1994.

Baskaran, M., Shaw, G.E., Residence time of Arctic haze aerosols using the concentrations and activity ratios of 210Po, 210Pb and 7Be., *Aerosol Science*, *32*, 443-452, 2001.

Brimblecombe, P., *Air composition & chemistry*, 253 pp., Cambridge University Press, Cambridge, 1996.

Carlson, T.N., Speculations on the movement of polluted air to the Arctic, *Atmospheric Environment*, *15* (8), 1473-1477, 1981.

Heintzenberg, J., What can we learn from aerosol measurements at baseline stations?, *Journal of Atmospheric Chemistry*, *3* (1), 153-169, 1985.

Heintzenberg, J., J. Strom, J.A. Ogren, and H.P. Fimpel, Vertical profiles of aerosol properties in the summer troposphere of Central Europe, Scandinavia and the Svalbard region, *Atmospheric Environment, Part A*, *25A* (3-4), 621-627, 1991.

IPCC, *Intergovernmental Panel on Climate Change*, Cambridge University Press, Cambridge, 1996.

Khattatov, V.U., A.E. Tyabotov, A.P. Alekseyev, A.A. Postnov, and E.A. Stulov, Aircraft lidar studies of the Arctic haze and their meteorological interpretation, *Atmospheric Research*, *44* (1-2), 99-111, 1997.

Lowenthal, D.H., R.D. Borys, and B.W. Mosher, Sources of pollution aerosol at Dye 3, Greenland, *Atmospheric Environment*, *31* (22), 3707-3717, 1997.

Oke, T.R., *Boundary Layer Climates*, 435 pp., Routledge, Cambridge, 1987.

Ottar, B., Gotaas, Y., Hov, O., Iversen, T., Joranger, E., Oehme, M., Pacyna, J., Semb, A., Thomas, W., Vitols, V., Air Pollutants in the Arctic, pp. 73, Norwegian Institute For Air Research, Lillestrom, 1986.

Pacyna, J.M., and B. Ottar, Transport and chemical composition of the summer aerosol in the Norwegian Arctic, *Atmospheric Environment*, *19* (12), 2109-2120, 1985.

Polissar, A.V., P.K. Hopke, P. Paatero, Y.J. Kaufmann, D.K. Hall, B.A. Bodhaine, E.G. Dutton, and J.M. Harris, The aerosol at Barrow, Alaska: long-term trends and source locations, *Atmospheric Environment*, *33* (16), 2441-2458, 1999.

Radke, L.F., J.H. Lyons, D.A. Hegg, P.V. Hobbs, and I.H. Bailey, Airborne observations of Arctic aerosols. I: characteristics of Arctic haze, *Geophysical Research Letters*, *11* (5), 393-396, 1984.

Rey, L., *The Arctic Ocean*, 433 pp., Macmillan Press LTD, London, 1982.

Seinfeld, J.H., *Atmospheric Chemistry and Physics*, 1326 pp., John Wiley & Sons, Inc., New York, 1998.

Strahler, A.H., Strahler, A.N., *Modern Physical Geography*, John Wiley & Sons, Inc, New York, 1992.

Svenningsson, B., Hygroscopic Growth of Atmospheric Aerosol Particles and Its Relation to Nucleation Scavering in Clouds, University of Lund, Lund, 1997.

Warneck, P., *Chemistry of the Natural Atmosphere*, 757 pp., Academic Press Inc. LTD, Londan, 1988.

Whitby, K.T., The Physaical Characteristics of Sulphur Aerosols, *Atmospheric Environment*, *12*, 135-159, 1978.

Xie, Y.L., P.K. Hopke, P. Paatero, L.A. Barrie, and S.M. Li, Identification of source nature and seasonal variations of Arctic aerosol by the multilinear engine, *Atmospheric Environment*, *33* (16), 2549-2562, 1999a.

Xie, Y.L., P.K. Hopke, P. Paatero, L.A. Barrie, and S.M. Li, Locations and preferred pathways of possible sources of Arctic aerosol, *Atmospheric Environment*, *33* (14), 2229-2239, 1999b.

INTERNET REFERENCES

1. *http://www1.tor.ec.gc.ca/*, Downloaded from the World Wide Web on the 15th of April.

2. http://res2.agr.gc.ca/, Downloaded from the World Wide Web on the 15th of April.

3. http://www.cfvh.kva.se/nspic23.html, Downloaded from the World Wide Web on the 21st of May 2001.

4. http://www.amap.no/assess/soaer3.htm#winter and spring, Downloaded from the World Wide Web on the 21st of May 2001.

5. http://www.nilu.no/niluweb/services/zeppelin/, Downloaded from the World Wide Web on the 15th of April.

6. http://zhou.pixe.lth.se. Downloaded from the World Wide Web on 5th of April.

7. http://gus.arlhq.noaa.gov/ready/hysplit4.html, Downloaded from the World Wide Web on the 15th of February 2001.

Appendix 1. Dates for trajectory calculations.

N	r3-4	deff a)mga små	b)få små	c)få små	S a)high	b)small	Va) Large	b)small
23-mar	02-maj	01-maj	18-mar	04-jun	21-mar	31-maj	21-mar	01-maj
24-mar	30-maj	02-maj	24-mar	05-jun	22-mar	08-jun	22-mar	06-maj
10-apr	03-jun	22-maj	12-maj	06-jun	23-mar	15-jun	23-mar	22-maj
24-apr	09-jun	14-jun	17-maj	15-jun	24-mar	24-jun	24-mar	01-jun
13-maj	19-jun	20-jun	25-maj	02-jul	30-mar	25-jun	30-mar	11-jun
16-maj	22-jun	22-jun	29-maj	06-jul	09-apr	03-jul	10-apr	13-jun
18-maj	02-jul	23-jun	26-okt	07-jul	10-apr	31-jul	11-apr	02-jul
30-maj	03-jul	25-jun	28-okt	09-jul	11-apr	01-aug	22-apr	08-jul
31-maj	17-jul	26-jun	01-nov	12-jul	21-apr	02-aug	13-maj	13-jul
20-jun	18-jul	18-jul	04-nov	17-jul	22-apr	09-aug	16-maj	21-jul
22-jun	25-jul	02-aug	05-nov	04-aug	23-apr	11-aug	19-maj	22-jul
23-jun	26-jul	03-aug	11-nov	06-aug	24-apr	20-aug	25-maj	31-jul
02-jul	28-jul	09-aug	12-nov	11-aug	12-maj	22-aug	27-maj	21-aug
11-jul	31-jul	20-aug	13-nov	16-aug	13-maj	30-aug	29-maj	22-aug
20-jul	09-aug	21-aug	14-nov	17-aug	14-maj	31-aug	30-maj	04-sep
21-jul	22-aug	30-aug	24-nov	18-aug	16-maj	21-sep	02-jul	17-sep
24-jul	23-aug	09-sep	25-nov	19-aug	17-maj	29-sep	16-aug	25-sep
05-aug	31-aug	05-okt	27-nov	29-aug	18-maj	05-okt	17-aug	30-sep
12-aug	04-sep	08-okt	08-dec	08-sep	19-maj	09-okt	09-okt	03-okt
17-aug	06-sep	19-jul	27-maj	28-sep	27-maj	10-okt	12-okt	29-okt
09-sep	21-sep	10-aug	20-mar	20-jun				
10-sep	28-sep	23-jul	15-maj	10-sep				
09-okt	08-okt	09-okt	12-jan	11-sep				
	18-okt							
	26-nov							
	28-nov							
	05-dec							

Lunds Universitets Naturgeografiska institution. Seminarieuppsatser. Uppsatserna finns tillgängliga på Naturgeografiska institutionens bibliotek, Sölvegatan 13, 223 62 LUND.

The reports are available at the Geo-Library, Department of Physical Geography, University of Lund, Sölvegatan 13, S-223 62 Lund, Sweden.

1. Pilesjö, P. (1985): Metoder för morfometrisk analys av kustområden.
2. Ahlström, K. & Bergman, A. (1986): Kartering av erosionskänsliga områden i Ringsjöbygden.
3. Huseid, A. (1986): Stormfällning och dess orsakssamband, Söderåsen, Skåne.
4. Sandstedt, P. & Wällstedt, B. (1986): Krankesjön under ytan - en naturgeografisk beskrivning.
5. Johansson, K. (1986): En lokalklimatisk temperaturstudie på Kungsmarken, öster om Lund.
6. Estgren, C. (1987): Isälvsstråket Djurfälla-Flädermo, norr om Motala.
7. Lindgren, E. & Runnström, M. (1987): En objektiv metod för att bestämma läplanteringars läverkan.
8. Hansson, R. (1987): Studie av frekvensstyrd filtringsmetod för att segmentera satellitbilder, med försök på Landsat TM-data över ett skogsområde i S. Norrland.
9. Matthiesen, N. & Snäll, M. (1988): Temperatur och himmelsexponering i gator: Resultat av mätningar i Malmö.

10A. Nilsson, S. (1988): Veberöd. En beskrivning av samhällets och bygdens utbyggnad och utveckling från början av 1800-talet till vår tid.

10B. Nilson, G., 1988: Isförhållande i södra Öresund.

11. Tunving, E. (1989): Översvämning i Murciaprovinsen, sydöstra Spanien, november 1987.
12. Glave, S. (1989): Termiska studier i Malmö med värmebilder och konventionell mätutrustning.
13. Mjölbo, Y. (1989): Landskapsförändringen - hur skall den övervakas?
14. Finnander, M-L. (1989): Vädrets betydelse för snöavsmältningen i Tarfaladalen.
15. Ardö, J. (1989): Samband mellan Landsat TM-data och skogliga beståndsdata på avdelningsnivå.
16. Mikaelsson, E. (1989): Byskeälvens dalgång inom Västerbottens län. Geomorfologisk karta, beskrivning och naturvärdesbedömning.
17. Nhilen, C. (1990): Bilavgaser i gatumiljö och deras beroende av vädret. Litteraturstudier och mätning med DOAS vid motortrafikled i Umeå.
18. Brasjö, C. (1990): Geometrisk korrektion av NOAA AVHRR-data.
19. Erlandsson, R. (1991): Vägbanetemperaturer i Lund.
20. Arheimer, B. (1991): Näringsläckage från åkermark inom Brååns dräneringsområde. Lokalisering och åtgärdsförslag.
21. Andersson, G. (1991): En studie av transversalmoräner i västra Småland.

22A. Skillius, Å., (1991): Water havesting in Bakul, Senegal.

22B. Persson, P. (1991): Satellitdata för övervakning av höstsådda rapsfält i Skåne.

23. Michelson, D. (1991): Land Use Mapping of theThat Luang - Salakham Wetland, Lao PDR, Using Landsat TM-Data.
24. Malmberg, U. (1991): En jämförelse mellan SPOT- och Landsatdata för vegetations-klassning i Småland.
25. Mossberg, M. & Pettersson, G. (1991): A Study of Infiltration Capacity in a Semiarid Environment, Mberengwa District, Zimbabwe.

26. Theander, T. (1992): Avfallsupplag i Malmöhus län. Dränering och miljöpåverkan.
27. Osaengius, S. (1992): Stranderosion vid Löderups strandbad.
28. Olsson, K. (1992): Sea Ice Dynamics in Time and Space. Based on upward looking sonar, satellite images and a time series of digital ice charts.
29. Larsson, K. (1993): Gully Erosion from Road Drainage in the Kenyan Highlands. A Study of Aerial Photo Interpreted Factors.
30. Richardson, C. (1993): Nischbildningsprocesser - en fältstudie vid Passglaciären, Kebnekaise.
31. Martinsson, L. (1994): Detection of Forest Change in Sumava Mountains, Czech Republic Using Remotely Sensed Data.
32. Klintenberg, P. (1995): The Vegetation Distribution in the Kärkevagge Valley.
33. Hese, S. (1995): Forest Damage Assessment in the Black Triangle area using Landsat TM, MSS and Forest Inventory data.
34. Josefsson, T. och Mårtensson, I. (1995). A vegetation map and a Digital Elevation Model over the Kapp Linné area, Svalbard -with analyses of the vertical and horizontal distribution of the vegetation.
35. Brogaard, S och Falkenström, H. (1995). Assessing salinization, sand encroachment and expanding urban areas in the Nile Valley using Landsat MSS data.
36. Krantz, M. (1996): GIS som hjälpmedel vid växtskyddsrådgivning.
37. Lindegård, P. (1996). Vinterklimat och vårbakslag. Lufttemperatur och kådflödessjuka hos gran i södra Sverige.
38. Bremborg, P. (1996). Desertification mapping of Horqin Sandy Land, Inner Mongolia, by means of remote sensing.
39. Hellberg, J. (1996). Förändringsstudie av jordbrukslandskapet på Söderslätt 1938-1985.
40. Achberger, C. (1996): Quality and representability of mobile measurements for local climatological research.
41. Olsson, M. (1996): Extrema lufttryck i Europa och Skandinavien 1881-1995.
42. Sundberg, D. (1997): En GIS-tillämpad studie av vattenerosion i sydsvensk jordbruksmark.
43. Liljeberg, M. (1997): Klassning och statistisk separabilitetsanalys av marktäckningsklasser i Halland, analys av multivariata data Landsat TM och ERS-1 SAR.
44. Roos, E. (1997): Temperature Variations and Landscape Heterogeneity in two Swedish Agricultural Areas. An application of mobile measurements.
45. Arvidsson, P. (1997): Regional fördelning av skogsskador i förhållande till mängd SO_2 under vegetationsperioden i norra Tjeckien.
46. Akselsson, C. (1997): Kritisk belastning av aciditet för skogsmark i norra Tjeckien.
47. Carlsson, G. (1997): Turbulens och supraglacial meandring.
48. Jönsson, C. (1998): Multitemporala vegetationsstudier i nordöstra Kenya med AVHRR NDVI
49. Kolmert, S. (1998): Evaluation of a conceptual semi-distributed hydrological model – A case study of Hörbyån.
50. Persson, A. (1998): Kartering av markanvändning med meteorologisk satellitdata för förbättring av en atmosfärisk spridningsmodell.
51. Andersson, U. och Nilsson, D. (1998): Distributed hydrological modelling in a GIS perspective – an evaluation of the MIKE SHE model.
52. Andersson, K. och Carlstedt, J. (1998): Different GIS and remote sensing techniques for detection of changes in vegetation cover - A study in the Nam

Ngum and Nam Lik catchment areas in the Lao PDR.

53. Andersson, J., (1999): Användning av global satllitdata för uppskattning av spannmålsproduktion i västafrikanska Sahel.
54. Flodmark, A.E., (1999): Urban Geographic Information Systems, The City of Berkeley Pilot GIS
55A. Lyborg, Jessic & Thurfell, Lilian (1999): Forest damage, water flow and digital elevation models: a case study of the Krkonose National Park, Czech Republic.
55B. Tagesson, I., och Wramneby, A., (1999): Kväveläckage inom Tolångaåns dräneringsområde – modellering och åtgärdssimulering.
56. Almkvist, E., (1999): Högfrekventa tryckvariationer under de senaste århundradena.
57. Alstorp, P., och Johansson, T., (1999): Översiktlig buller- och luftföroreningsinventering i Burlövs Kommun år 1994 med hjälp av geografiska informationssystem – möjligheter och begränsningar.
58. Mattsson, F., (1999): Analys av molnklotter med IRST-data inom det termala infraröda våglängdsområdet
59. Hallgren, L., och Johansson, A., (1999): Analysing land cover changes in the Caprivi Strip, Namibia, using Landsat TM and Spot XS imagery.
60. Granhäll, T., (1999): Aerosolers dygnsvariationer och långväga transporter.
61. Kjellander, C., (1999): Variations in the energy budget above growing wheat and barley, Ilstorp 1998 - a gradient-profile approach
62. Moskvitina, M., (1999): GIS as a Tool for Environmental Impact Assessment - A case study of EIA implementation for the road building project in Strömstad, Sweden
63. Eriksson, H., (1999): Undersökning av sambandet mellan strålningstemperatur och NDVI i Sahel.
64. Elmqvist, B., Lundström, J., (2000): The utility of NOAA AVHRR data for vegetation studies in semi-arid regions.
65. Wickberg, J., (2000): GIS och statistik vid dräneringsområdesvis kväveläckagebeskrivning i Halland.
66. Johansson, M., (2000): Climate conditions required for re-glaciation of cirques in Rassepautasjtjåkka massif, northern Sweden.
67. Asserup, P., Eklöf, M., (2000): Estimation of the soil moisture distribution in the Tamne River Basin, Upper East Region, Ghana.
68. Thern, J., (2000): Markvattenhalt och temperatur i sandig jordbruksmark vid Ilstorp, centrala Skåne: en mätnings- och modelleringsstudie.
69. Andersson, C., Lagerström, M., (2000): Nitrogen leakage from different land use types - a comparison between the watersheds of Graisupis and Vardas, Lithuania.
70. Svensson, M., (2000): Miljökonsekvensbeskrivning med stöd av Geografiska Informationssystem (GIS) – Bullerstudie kring Malmö-Sturup Flygplats.
71. Hyltén, H.A., Uggla, E., (2000): Rule.Based Land Cover Classification and Erosion Risk Assessment of the Krkonoše National Park, Czech Republic.
72. Cronquist, L., Elg, S., (2000): The usefulness of coarse resolution satellite sensor data for identification of biomes in Kenya.
73. Rasmusson, A-K., (2000): En studie av landskapsindex för kvantifiering av rumsliga landskapsmönster.
74. Olofsson, P., Stenström, R., (2000): Estimation of leaf area index in southern Sweden with optimal modelling and Landsat 7 ETM+Scene.
75. Uggla, H., (2000): En analys av nattliga koldioxidflöden i en boreal barrskog avseende spatial och temporal variation.

76. Andersson, E., Andersson, S., (2000): Modellering och uppmätta kväveflöden i energiskog som bevattnas med avloppsvatten.
77. Dawidson, E., Nilsson, C., (2000): Soil Organic Carbon in Upper East Region, Ghana - Measurements and Modelling.
78. Bengtsson, M., (2000): Vattensänkningar - en analys av orsaker och effekter.
79. Ullman, M., (2001): El Niño Southern Oscillation och dess atmosfäriska fjärrpåverkan.
80. Andersson, A., (2001): The wind climate of northwestern Europe in SWECLIM regional climate scenarios.
81. Lalloo, D., (2001): Geografiska informationssystem för studier av polyaromatiska kolväten (PAH) – Undersökning av djupvariation i BO01-området, Västra hamnen, Malmö, samt utveckling av en matematisk formel för beräkning av PAH-koncentrationer från ett kontinuerligt utsläpp.
82. Almqvist, J., Fergéus, J., (2001): GIS-implementation in Sri Lanka.
Part 1: GIS-applications in Hambantota district Sri Lanka : a case study.
Part 2: GIS in socio-economic planning : a case study.
83. Berntsson, A., (2001): Modellering av reflektans från ett sockerbetsbestånd med hjälp av en strålningsmodell.
84. Umegård, J., (2001): Arctic aerosol and long-range transport.